Journal of
Composites Science

MDPI

Review

Transforming Nanomaterial Synthesis through Advanced Microfluidic Approaches: A Review on Accessing Unrestricted Possibilities

Sanjib Roy [1,†], Ramesh Kumar [2,*], Argha Acooli [1], Snehagni Roy [1], Abhrajit Chatterjee [1], Sujoy Chattaraj [3], Jayato Nayak [4], Byong-Hun Jeon [2,*], Aradhana Basu [5], Shirsendu Banerjee [1,†], Sankha Chakrabortty [1,†] and Suraj K. Tripathy [1]

[1] School of Chemical Engineering, Kalinga Institute of Industrial Technology, Bhubaneswar 751024, India; roysanjib70@gmail.com (S.R.); arghatuhinacooli@gmail.com (A.A.); snehagniroy16@gmail.com (S.R.); abhrajit.chatterjee@gmail.com (A.C.); shirsendu.banerjee@kiitbiotech.ac.in (S.B.); sankha.chakrabortty@kiitbiotech.ac.in (S.C.); suraj.tripathy@kiitbiotech.ac.in (S.K.T.)
[2] Department of Earth Resources & Environmental Engineering, Hanyang University, 222-Wangsimni-ro, Seongdong-gu, Seoul 04763, Republic of Korea
[3] Department of Chemical Engineering, Indian Institute of Technology Madras, Chennai 600036, India; chattaraj.sujoy@gmail.com
[4] Centre for Life Science, Mahindra University, Hyderabad 500043, India; nayak.jayato@gmail.com
[5] School of Sustainability, XIM University, Bhubaneswar 752050, India; aradhanabasu902@gmail.com
* Correspondence: rameshibt@gmail.com or rameshibt@hanyang.ac.kr (R.K.); bhjeon@hanyang.ac.kr (B.-H.J.)
† These authors contributed equally to this work.

Abstract: The inception of microfluidic devices marks a confluence of diverse scientific domains, including physics, biology, chemistry, and fluid mechanics. These multidisciplinary roots have catalyzed the evolution of microfluidic devices, which serve as versatile platforms for various chemical and biological processes. Notably, microfluidic devices have garnered attention as efficient reactors, offering distinct benefits such as minimized spatial requirements for reactions, reduced equipment costs, and accelerated residence times. These advantages, among others, have ignited a compelling interest in harnessing microfluidic technology for the conception, refinement, and production of various nanomaterials and nanocomposites, pivotal within both industrial and medicinal sectors. This comprehensive exposition delves into multifaceted aspects of nanomaterial synthesis, underscoring the transformative role of microfluidic methodologies as a departure from conventional techniques. The discourse navigates through intricate considerations surrounding the preparation of nanomaterials, elucidating how the microfluidic paradigm has emerged as a promising alternative. This paper serves as an illuminating exploration of the juncture between microfluidic innovation and nanomaterial synthesis. It traverses the transformative potential of microfluidics in revolutionizing traditional approaches, heralding a new era of precision engineering for advanced materials with applications spanning industrial to medicinal domains.

Keywords: nanomaterials; synthesis processes; microfluidic process; cost-effective

Citation: Roy, S.; Kumar, R.; Acooli, A.; Roy, S.; Chatterjee, A.; Chattaraj, S.; Nayak, J.; Jeon, B.-H.; Basu, A.; Banerjee, S.; et al. Transforming Nanomaterial Synthesis through Advanced Microfluidic Approaches: A Review on Accessing Unrestricted Possibilities. *J. Compos. Sci.* **2024**, *8*, 386. https://doi.org/10.3390/jcs8100386

Academic Editor: Giuseppe Cavallaro

Received: 22 August 2024
Revised: 15 September 2024
Accepted: 23 September 2024
Published: 25 September 2024

1. Introduction

Nanomaterials represent a fascinating class of substances sought after for their diverse practical applications. Defined by their size falling within the 1 to 100 nm range, these materials hold immense promise across various fields. Fabricating nanomaterials involves employing various methods tailored to their specific types and properties. The two primary approaches used for their development are the "top-down" and "bottom-up" methods, as illustrated in Figure 1 below [1]. In the bottom-up approach, materials are built atom by atom or molecule by molecule, ultimately forming nanoparticles (NPs). This process often begins at the atomic scale, where nucleation occurs, forming nanoscale structures.

Conversely, the top-down method involves breaking down larger bulk materials into nano-sized entities [2]. Techniques such as mechanical milling, laser ablation, etching, sputtering, and electro-explosion are commonly utilized in top-down methodologies to achieve this size reduction [3]. The bottom-up approach allows for precise control over the structure and composition of nanomaterials, enabling the design of novel materials with tailored properties. It offers opportunities for engineering complex nanostructures with specific functionalities, such as catalytic activity, optical properties, and mechanical strength [4]. This method is particularly useful for applications requiring uniformity and scalability, such as nanoelectronics and drug delivery systems. On the other hand, the top-down approach is advantageous for transforming existing bulk materials into nanoscale counterparts. This method is often employed when starting with abundant, readily available materials, allowing for cost-effective production of nanomaterials on a large scale. However, it may present challenges in achieving uniform size distribution and controlling the properties of the resulting nanoparticles. Nanomaterials hold immense potential due to their unique size-dependent properties, with applications ranging from electronics to medicine. Understanding and harnessing the capabilities of both bottom-up and top-down fabrication methods are crucial for advancing nanotechnology and unlocking new opportunities in various industries.

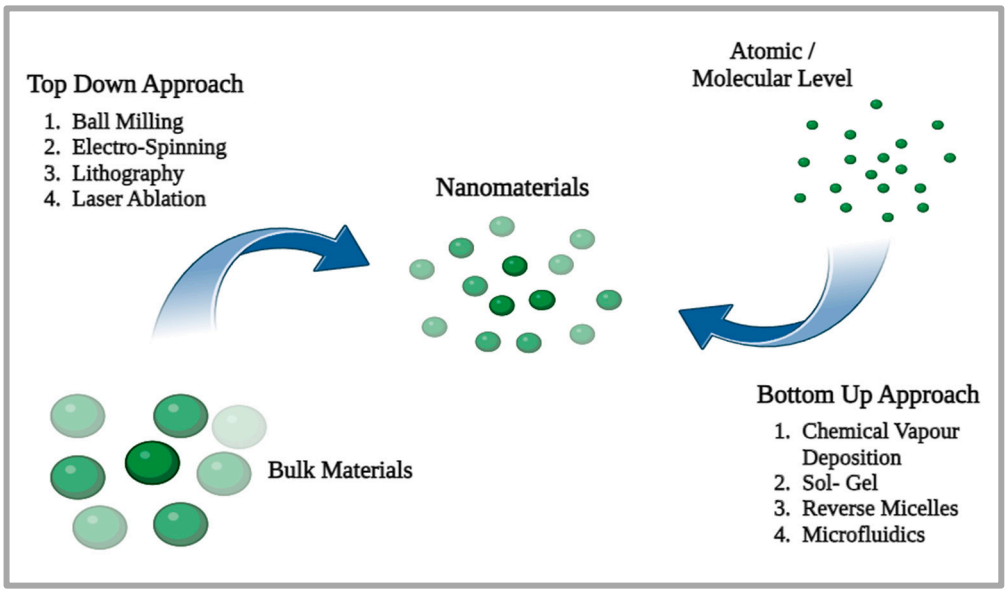

Figure 1. The two conventional approaches in the fabrication of nanomaterials.

The importance of nanotechnology increased after the discovery that a major contributing factor to a material's property is its size. After that, different methods to produce nanomaterials have been employed worldwide. Some include hydrothermal synthesis, chemical precipitation, and condensation [5–7]. However, suitable synthesis routes are important for reaching the desired product quality and application. As a result, a newer technology like microfluidics emerged [8].

Minimizing the synthesis process using microfluidic channels is an alternate strategy to traditional approaches. Whitesides states that microfluidics is the learning and advancement of devices for processing or manipulating minimal fluid quantity (10^{-9} to 10^{-18} L) through channels 10 to 100 μm in diameter [9]. Due to their micro-scale dimensions and mixing, fine control over flow parameters, tunability of particle size, and repeatability, microchannels provide an alternative to top-down techniques and bulk mixing [10]. In microfluidic technology, fluid flow is precisely controlled in microchannels with various diameters and shapes, from micrometers to millimeters. Most important unit operations, like heat transfer, mass transfer, mixing of fluids, typical automation, and residence time

distribution are improved due to the geometric shapes and dimensions of the microfluidic devices [11–13]. Moreover, microfluidic NPs are affected by several variables, including temperature, precursor concentration, duration, and pH, much like bulk mixing of bottom-up techniques. Nevertheless, because microfluidics operate continuously, other variables like residence time, total flow rate (TFR), and flow rate ratio (FRR) also affect these variables and the physicochemical characteristics of NPs [14]. These merits of the microfluidic method compared to conventional methods have guided further research in designing and fabricating low-cost, disposable, and portable microfluidic devices [12]. The above distinctiveness comes into play in applications in biological, chemical, pharmaceutical, clinical, medicinal, and other diverse fields of industrial technologies [15,16]. Another advantage of microfluidic methods is that they mitigate major challenges related to scale-up reactors. The preparation of nanoparticles and chemical synthesis in these reactors are extensively done using microfluidic methods [17,18]. This technique has emerged with tremendous potential in many fields, including biomedical applications [19,20], controlled drug delivery [21–24], biosensors [25], and energetic materials such as nano 2,6-diamino-3,5-dinitropyrazine-1-oxide (LLM-105) [26].

This article provides a critical comparative analysis of the conventional approaches and microfluidic techniques used for nanoparticle synthesis, which is quite missing in other recent studies [27,28]. It explores the wide diversity of materials that can be produced using microfluidics and their possible uses. The specific mechanisms employed in microfluidic systems, such as the Single-Phase Flow (Continuous-Flow) and Multi-Phase Flow (Droplet-Based) Systems, were also highlighted in this article. Although conventional techniques have been widely employed in the fabrication of nanomaterials, microfluidic approaches have unique benefits. Using microfluidics, reaction conditions may be precisely controlled, resulting in homogenous nanoparticles, nanowires, and nanostructures with various functionalities. The study thoroughly examines this feature, highlighting the effectiveness and adaptability of microfluidic techniques. The report also explores the possible uses of nanomaterials produced via microfluidics in various disciplines. These materials can potentially improve electrical device performance and facilitate the creation of new components. They have the potential to increase sustainability and efficiency in energy applications. In addition, medication transport, diagnostics, and treatments can all be revolutionized in medicine by microfluidic-generated nanomaterials. It provides ways to protect the environment by identifying and eliminating pollution. The revolutionary potential of microfluidic technologies is emphasized in contrast with conventional approaches. Microfluidic procedures provide scalability, reproducibility, and exact control over the creation of intricate structures. They have the power to completely transform the synthesis of nanomaterials, resulting in breakthroughs in science and creativity. In a nutshell, this paper is an invaluable tool for learning about the synthesis of nanomaterials and how microfluidic techniques may influence the development of numerous sectors in the future. It looks at the pros and cons of both methods and covers the many uses for nanomaterials produced by microfluidic processes. It emphasizes the profound influence these developments may have on electronics, energy, health, and environmental preservation, advancing the transition to a more technologically sophisticated and sustainable future. Furthermore, staying updated with all the latest achievements and trends in this field of study is crucial, considering the quick advances in nanoparticle synthesis and application potential.

2. Methods of Preparation of Nanomaterials

Nanomaterials have become incredibly useful across many fields, especially in medicine, where they are used in biosensors, targeted drug delivery systems, diagnostic tools, and therapeutic devices. As a result of this, there is a growing need for nanomaterial synthesis methods that are not only effective but also affordable and tailored to specific applications in these areas [18,29]. Figure 1 illustrates various approaches to the fabrication of nanostructures. In the top-down approach, the primary focus is reducing the size, achieved

through mechanical actions like grinding or milling. While this method is often favored for large-scale industrial processes, the associated equipment and energy costs can make it economically impractical. On the flip side, the bottom-up approach involves the growth and aggregation of nanostructures, requiring less mechanical force and energy. This method typically yields amorphous particles with enhanced solubility properties. It is faster, simpler, and more cost- and energy-efficient, making it well-suited for small-scale nanoparticle production with highly uniform size distributions [17]. Figure 2 showcases various techniques for synthesizing nanoparticles, offering a comprehensive overview of available methods.

Although several techniques are available, as seen in Figure 2, there is a vast difference between expected and produced nanomaterials. This may be due to several reasons, like improper selectivity and yielding improper product-controlling parameters [30]. Although we may get nanoparticles of uniform size through chemical and physical processes, the impact of these on the environment cannot be overlooked. This is because of the excess hazardous and toxic materials released into the environment [31,32]. They act as environmental pollutants, especially land and water pollutants [33]. Apart from that, the requirement for huge areas, high-cost equipment, and high power consumption add to the high capital investments [34]. Some other issues during scale-up are changes in conditions required for synthesis, improper mixing of the reactants or raw materials during production, sequential operations being very complex, high percentage of waste produced, safety considerations, and poor reproduction of the results, particular working conditions of the equipment and very long residence time [30,35].

Moreover, there is a good chance of agglomeration of synthesized products due to uncontrolled growth (due to size distribution discrepancies) [36], a huge chance of contamination [17], the non-uniform structure of the surface [32], and improper size distributions [37]. These disadvantages hinder the whole chemistry or chemical process initially aimed at green synthesis and precision biomedicine [30]. Another limitation of the synthesis process is that the path from research to applications is prolonged, especially in medicine [38,39]. This has caused an urgent need to develop efficient and easy-to-change techniques for synthesizing high-quality nanomaterials [40].

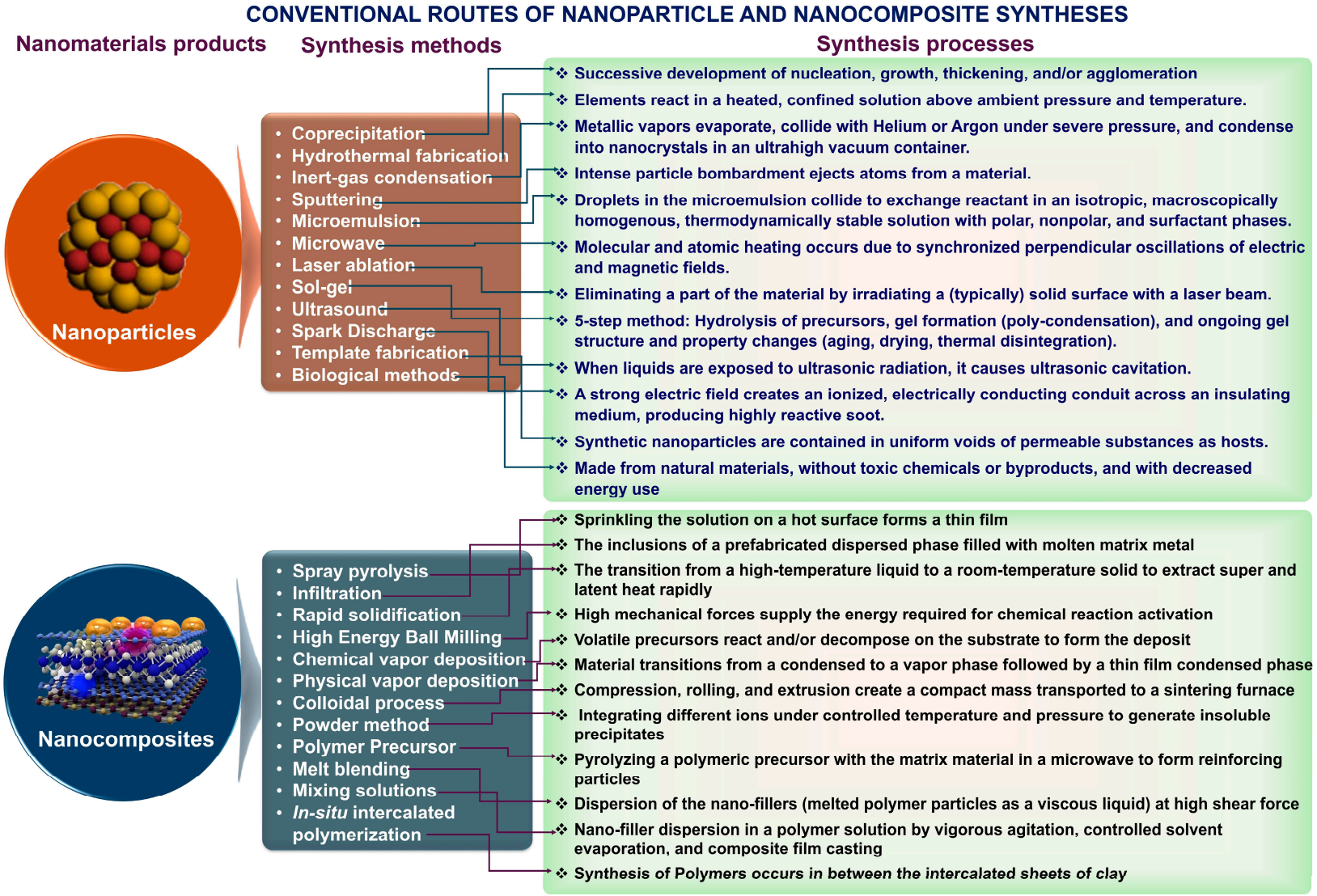

Figure 2. Nanocomposites and nanoparticles fabrication using different traditional methods [Adapted from [41]].

3. Conventional Methods Used in the Synthesis of Nanomaterials

3.1. The Top-Down Method

The top-down method divides most of the material into nanoscale structures or particles. The methods used to create micron-sized particles have been extended to create the top-down synthesis. Top-down methods are fundamentally simpler, relying on eliminating, dividing bulk material, or miniaturizing bulk manufacturing procedures to create the required structure with the right attributes.

3.1.1. Mechanical Milling (Ball Milling)

Mechanical milling is a potent technique for crafting nanoscale materials from bulkier counterparts. It serves as an efficient avenue for producing nanocomposites or blends of different phases, facilitating the creation of various materials like wear-resistant spray coatings, Al/Ni/Mg/Cu-based nanoalloys, and aluminum alloys fortified with oxide and carbide [42]. This process utilizes a high-energy mill (Figure 3), introducing a specific powder charge and milling medium [43,44]. The kinetic energy derived from the movement of the balls within the mill is imparted to the powder charge, disrupting chemical bonds, linking constituent molecules, and diminishing particle size. Several processes, such as the exchange of energy and mass and the generation of mechanical stress as an outcome of milling, lead to the shattering of the materials' matrix structure [43]. The ball milling process influences crystal deformation, a greater defect density, and increased material temperatures. The particular type of mill, the powder used that drives the milling chamber, the milling speed, the dimension and distribution of the balls, whether the mill is dry or wet, the temperature during the milling process, and the length of the milling process are all factors that affect how much energy is transferred [45]. The balls' kinetic energy is a function of their velocity and mass; steel or tungsten carbide balls are preferred over ceramic balls and are optimized according to size and size distribution [46].

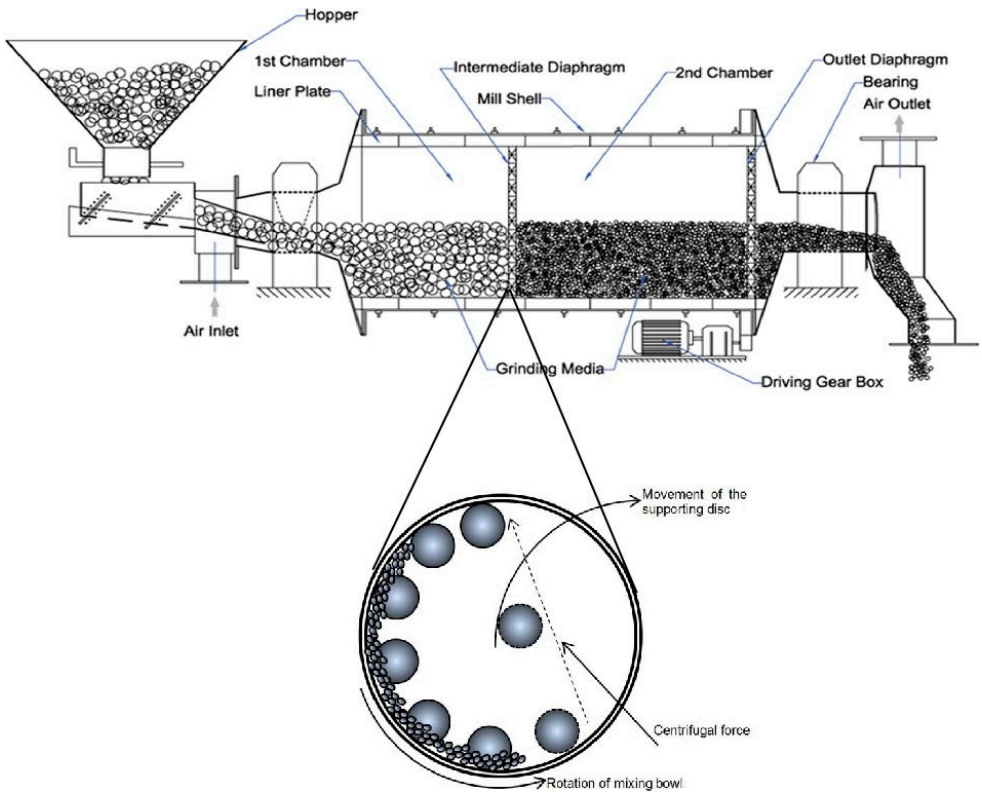

Figure 3. A ball mill process is used to generate nanoparticles (cross-sectional view and lateral view) [43,44].

As studied by Mei and Lu [47], the balls' kinetic energy, the properties of the milling media, and the powder affect the temperature throughout the milling process. The powder temperature influences its diffusivity and defect concentration, which affects the phase changes brought on by milling. Due to safety concerns or potentially harmful chemical effects on human health, physical procedures are recommended over enzymatic or chemical methods for producing SNP. Additionally, chemical processes take more time and include additional purification stages; in contrast, physical approaches are considered secure and environmentally beneficial [38].

3.1.2. Electrospinning

One of the most straightforward top-down approaches to developing nanostructured materials is electrospinning. It is a primary approach for creating continuous nanofibrous materials from an array of materials, which has benefits, including easy device manufacturing, material compatibility, and adjustable fiber shape [42,48]. High surface area-to-volume ratios, tunable surface shape, and accurate alignment are all characteristics of electrospun fibers. Coaxial electrospinning was a significant advancement in the field of electrospinning. This top-down method is efficient and practical to produce core-shell ultra-thin fibers on an industrial scale. These very thin nanomaterials have lengths that may be expanded to many centimeters. Inorganic, organic, and hybrid materials, as well as core-shell and hollow polymers, have all been developed using this technique [48].

In nanotechnology, electrospinning techniques come in a variety of forms. Here are a few methods that are often used:

Conventional electrospinning involves using a grounded collector, a syringe or spinneret filled with a polymer solution, and a high-voltage power source. A thin stream of polymer fluid is ejected from the spinneret into the collector until it solidifies into a fiber, overcoming viscosity forces with the application of high voltage. Coaxial electrospinning, on the other hand, simultaneously electrospins at least two solutions through concentrically organized spinnerets. Typically, a core fluid (such as a medication solution) and a shell fluid (like a polymer solution) are used. This technique allows for incorporating multiple components or the controlled release of functional elements within the fiber's core. Fe_3O_4 NPs were produced with various saturation magnetization (Ms) values. The surface of Fe_3O_4 nanoparticles can be changed to increase specific qualities. The research team of Song synthesized Fe_3O_4-polyhedral oligomeric silsesquioxane (POSS) particles using hydrosilylation, preserving a Ms value of 18.77 emu g1. The POSS improved surface potential stability and charge retention in the materials [49].

Owing to the magnetic anisotropy that exists in materials, the geometry of magnetic substances significantly impacts their characteristics. Therefore, it is crucial to investigate how the aligned fiber is made and how the distribution of its domains changes. The hydrothermal process and electrospinning method were used to create nanoparticles and nanofibers, respectively [50]. Cheng synthesized nanofibers in different drums of varying width and diameter and found out that the average diameter of nanofibers was 94.6 mm to 99.8 mm. The drum, which had a width of 4 cm and a diameter of 7 cm, did not produce aligned nanofibers. In contrast, the drum with a width of 2 cm and a diameter of 7 cm had significantly more orientation as the reduction in the width of the collecting tube made the electric field distribution more centralized [50]. Figure 4 shows a schematic representation of the electrospinning apparatus used to generate nanoparticles.

This structure makes the development of core-shell nano architectures with diverse properties and functionalities possible when subjected to an electric field. Coaxial electrospinning has become increasingly popular as a top-down process that is both efficient and uncomplicated by design to produce core-shell ultrathin fibers on a wide scale. In addition to having consistent dimensions, the fibers produced by this technology can also reach lengths that extend to several centimeters, making them suitable for a wide range of uses in the industrial sector. The fabrication of a wide variety of materials, such as core-shell and hollow polymer fibers, as well as inorganic, organic, and hybrid nanomaterials, has

been accomplished with great success through this technological approach [51]. By having the capacity to change the composition of both the core and shell materials, it is possible to construct fibers with features that may be tuned to specific needs. These properties may include higher thermal stability, increased mechanical strength, or controlled release in drug delivery systems. Consequently, coaxial electrospinning has developed into a versatile technique with applications in various sectors, such as materials science, biology, and nanotechnology [52].

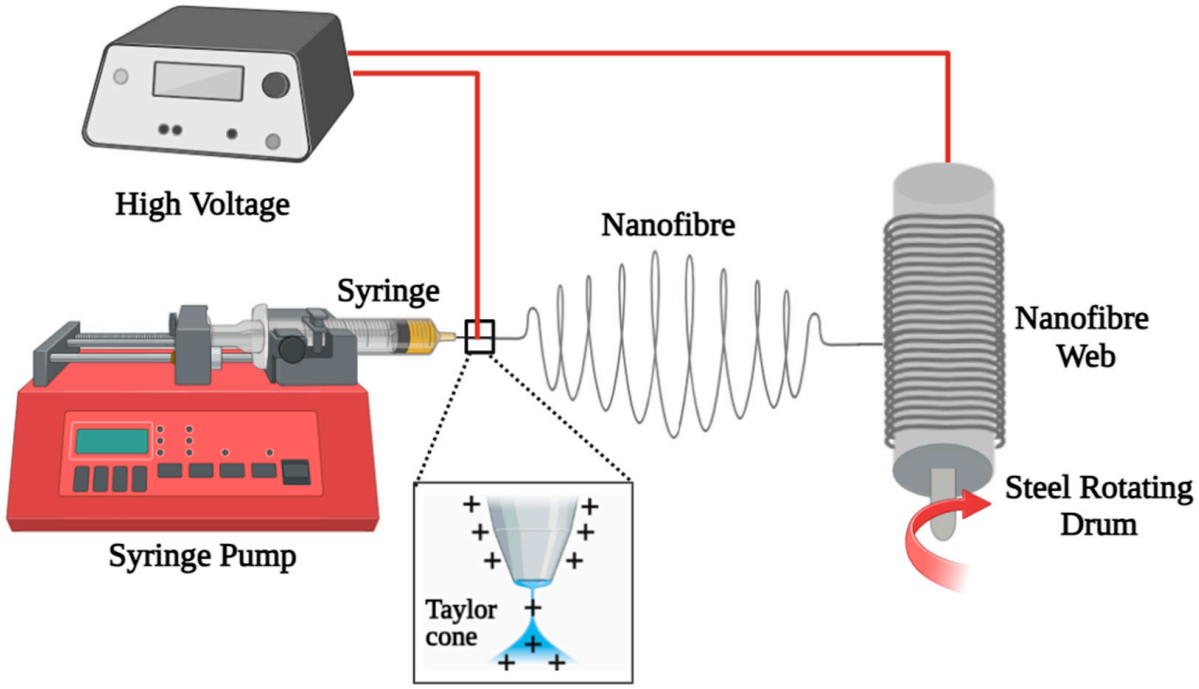

Figure 4. Basic parts of an electrospinning apparatus are used to generate nanoparticles.

3.1.3. Lithography

Lithography is a technique used to create images by immersing a substrate, typically stamped with an image, into ink. Various parts of this stamp have hydrophobic and hydrophilic properties; the former soaks up ink while the latter pushes it away. Patterns that resemble those on the substrate itself are frequently reproduced by this method. Surfaces are patterned using various lithographic techniques, such as photolithography, ultraviolet (UV), electronic beam, scanning probe, soft, and nano-lithography [42,53]. Techniques like scanning tunneling microscopy (STM) and atomic force microscopy (AFM) use a sharp probe to directly alter or eliminate materials from a substrate's surface. This allows for the exact fabrication of structures at the nanoscale with control down to the individual atom or molecule. Electron beam lithography (EBL) utilizes a concentrated electron beam to shape the substrate, offering superior resolution compared to optical lithography, although it tends to be slower. A resist-coated substrate is scanned by the electron beam to produce the desired pattern, achieving high resolution down to 10 nm but with slower processing times. Nanolithography (NL) deforms a resist mechanically to create a pattern: a resist-coated substrate is pressed into templates, causing the resist to copy the design onto the substrate. NL allows for high-resolution and large-area patterning.

The techniques of photolithography [54], nanoimprint lithography [55], and soft lithography [56] are all included in the masked lithography process. For example, scanning probes, focused ion beams, and electron beam lithographies are examples of maskless lithography. Writing arbitrary nanopatterns is carried out without a mask with maskless lithography. Ion implantation with a focused ion beam in conjunction with wet

chemical etching is a method that can be utilized to form three-dimensional freeform micro-nano-fabrication.

3.1.4. Laser Ablation

The laser ablation method creates nanoparticles by subjecting the target material to a powerful laser beam. This intense laser irradiation causes the original material or precursor to vaporize, forming noble metal nanoparticles. This method is environmentally friendly because it requires no stabilizing agents or additional chemicals. Moreover, laser ablation offers numerous advantages, such as precise control, high resolution, and versatility in processing nanomaterials. These qualities make it a sustainable option for generating noble metal nanoparticles with minimal environmental impact. This method can synthesize various materials like ceramics, metal nanoparticles, carbon nanoparticles, and so on [1,42,57].

Laser ablation offers a versatile approach for various applications: (a) Synthesis of Nanoparticles involves ablating a substance in a gaseous or liquid environment to create nanoparticles, ejected due to the laser beam's interaction, with adjustable size, composition, and shape through laser and material parameter manipulation. (b) Surface Modification and Functionalization utilize laser ablation to alter surface properties like wettability, chemical composition, and roughness, enabling surface texturing, biofunctionalization, and tailored micro- or nanostructures. (c) Nanoscale Fabrication employs laser ablation for precise material removal or deposition, facilitating the development of nanoscale structures, tools, and sensors essential in manufacturing microelectronics, integrated circuits, and microfluidic devices.

A hybrid composition of silver nanoparticles (AgNPs) and copper oxide nanoparticles (CuONPs) was utilized in the research carried out by Ahmed et al. to synthesize graphene oxide (GO) nanosheets that were favorable to the environment [38]. The utilization of the Pulsed Laser Ablation methodology accomplished this. Through green laser ablation, the procedure involved the distribution of copper and silver oxide nanoparticles onto graphene oxide nanosheets. A pulse duration of 7 nm, a repetition rate of 10 hertz, and a power of 3.6 watts were all characteristics utilized by the Nd:YAG nanosecond laser source. Initially, a silver disc weighing 10 g and having a purity level of 99.99% was placed in a beaker that contained 50 mL of deionized water and 0.5 g of graphite oxide (GO). To produce AgNPs@GO, perfect silver nanoparticles (AgNPs) were present in the GO suspension. This was accomplished by delivering a nanosecond laser beam in a direction that was perpendicular to the silver target. Similarly, pure copper oxide nanoparticles, known as CuONPs, were produced in the GO suspension, forming CuONPs@GO. These suspensions of AgNPs@GO and CuONPs@GO were then centrifuged and dried at a temperature of 60 °C for 4 hours. In transmission electron micrographs, graphene oxide was found to be generated in nanolayers that were broader than 350 nm. On the other hand, AgNPs and CuONPs were seen to be spherical shapes, with diameters ranging from 3.5 to 27.3 nm and 5.3 to 13.6 nm, respectively. An illustration of the standard procedure utilized for the production of nanoparticles employing the laser ablation method can be found in Figure 5 [58,59].

The laser pulses interact with the material that is submerged in a liquid, which results in the vaporization of the substance and the subsequent production of nanoparticles in the liquid medium using this technique. The ability to regulate and tailor the attributes of the nanoparticles, such as their average size and size distribution, is one of the most significant advantages of the PLAL technique. This is accomplished by altering the optical parameters of the laser. Various factors can strongly impact the outcome, including the laser fluence (energy per unit area), the wavelength, and the presence of salts or other modifiers in the liquid during the process [60]. Research has demonstrated that the sizes of manufactured nanoparticles, such as palladium (Pd) nanoparticles, are especially sensitive to changes in the considered factors. By way of illustration, for instance, raising the fluence or altering the wavelength of the laser can result in nanoparticles that are either smaller or larger,

respectively [61]. Since it allows for such a great degree of control over the properties of nanoparticles, laser ablation is a very versatile and valuable technology in nanomaterial synthesis, which may be applied in a wide variety of scientific and industrial fields.

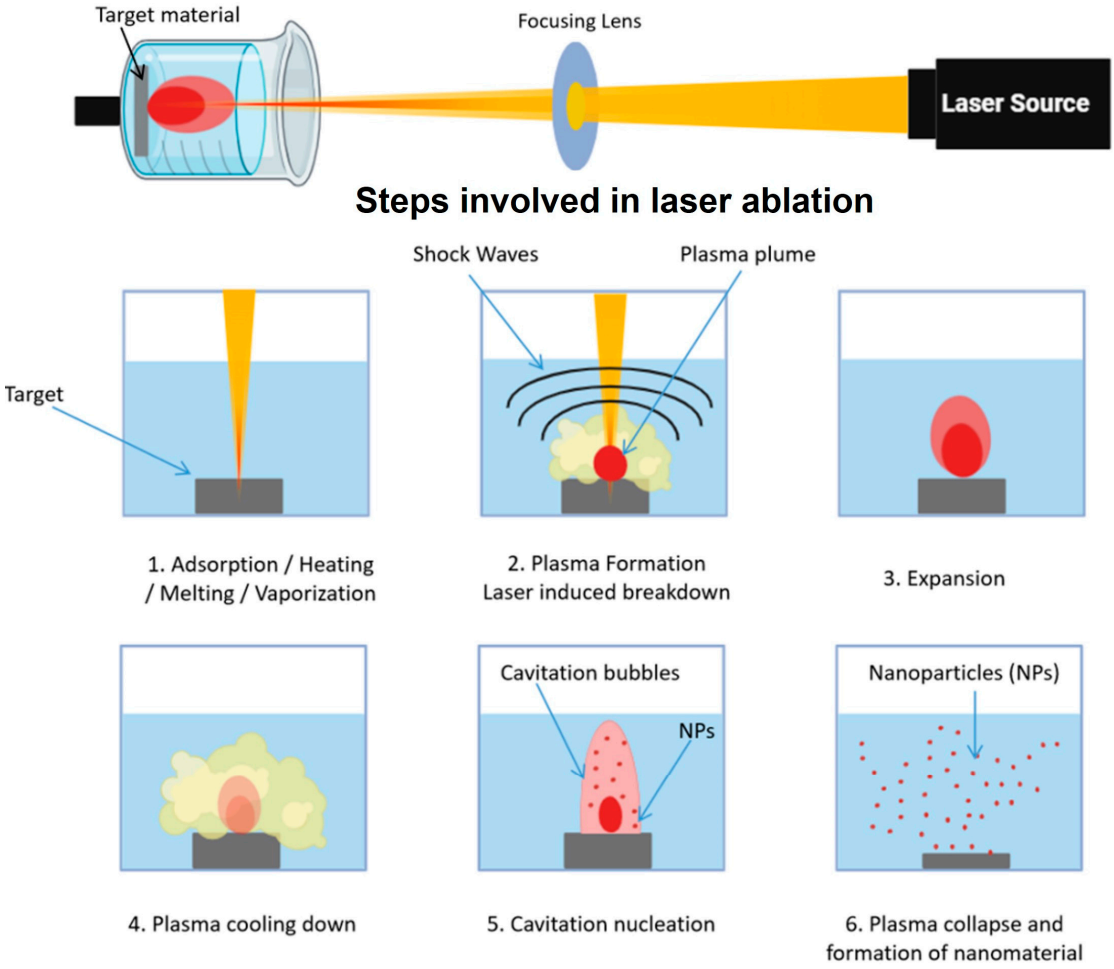

Figure 5. Schematic representation of nanoparticle synthesis in laser ablation process [58,59].

3.1.5. Sputtering Method

The sputtering process involves hitting solidified surfaces with high-energy particles, like gas or plasma, to create nanomaterials. Sputtering is a well-respected technique for creating nanomaterial thin films. Sputtering deposition involves the physical ejection of tiny atom clusters, depending on the incident gaseous-ion energy, from the target surface due to intense gaseous ions bombarding the surface [62,63]. Various methods for conducting sputtering include magnetron, radio-frequency diode, and DC diode sputtering. The sputtering method is typically done in a chamber evacuated before introducing the sputtering gas. Collecting gas ions requires applying a high voltage to the cathode target, which causes free electrons to collide with the gas. The positively charged ions repeatedly strike the cathode target as they speed towards it in the electric field, causing atoms to be ejected off the surface of the target [64]. SiO_2 and carbon paper substrates can be coated with WSe_2-layered nanofilms using magnetron sputtering [65]. An intriguing aspect of the sputtering approach is that, in contrast to electron-beam lithography, it is both cost-effective and produces nanomaterials with a composition identical to the target material but with fewer imperfections [66].

3.1.6. The Arc Discharge Method

Many nanostructured materials can be produced using the arc discharge technique. Its primary contribution to the material science community has been the creation of carbon-based compounds and materials, including fullerenes, CNHs, CNTs, FLG, and amorphous circular carbon nanoparticles [67]. The arc discharge technique is quite important for creating fullerene nanomaterials. The formation process involves manipulating two graphite rods within a cylinder that maintains a specific helium pressure. Oxygen or moisture prevents fullerene production; hence, filling the chamber with pure helium is crucial. The arc discharge between the graphite rod ends is the driving force behind the vaporization of carbon rods [68]. The arc discharge method involves collecting carbon-based nanomaterials from various sites due to their varying development methods. Different materials, such as MWCNTs, pyrolytic graphite, nano-graphite, high-purity polyhedral graphite, and other similar particles in deposits are made at the cathode, anode, or even both [69,70]. It is possible to extract carbon-based nanomaterials from the inner chamber in addition to the electrodes. Various atmospheric conditions can lead to the formation of single-wall carbon nanohorns (SWCNHs) with varying morphologies. One example is the production of "bud-like" SWCNHs in CO and CO_2 environments, as opposed to "dahlia-like" SWCNHs in an ambient atmosphere [71]. Graphene nanostructures may be efficiently created using the arc discharge process. The properties of graphene can be influenced by the conditions present during its synthesis. Graphene sheets produced by hydrogen arc discharge exfoliation outperform their argon arc discharge counterparts in electrical conductivity and thermal stability [72].

3.2. The Bottom-Up Method

The alternate strategy is called "bottom-up," which can produce less waste and is thus more cost-effective. It is a buildup method where a nanoparticle is obtained by conjugating one or more nanoparticles. The majority of these techniques are still under development. The most common bottom-up methods include sol-gel synthesis, hydrothermal synthesis, and micro fluidic approach. Due to numerous advantages, including fewer flaws, increased homogeneous chemical composition, and comparatively better ordering, the bottom-up technique is often used to produce nanoparticles.

3.2.1. Chemical Vapor Deposition (CVD)

Surfaces can be coated with solid byproducts of chemical vapor deposition, which involves transforming volatile precursors into solids through a chemical reaction [73]. Deposition of powders or films necessitates either gas-phase homogeneous chemical processes or surface- or near-surface heterogeneous chemical reactions (Figure 6) [40,74]. Energy must be supplied to the system for it to react during most CVD processes, which are thermodynamically endothermic [74,75]. Thanks to methods like atomic layer deposition (ALD), vapor-liquid, and solid growth, which can regulate the growth process at the nanoscale, CVD strategies have played a significant role in advancing cutting-edge technology. The development of nanotechnology has only reinforced their importance [76]. CVD synthesis involves several key steps: (a) Precursor Selection, where appropriate precursor molecules are chosen based on the desired nanoparticle composition; (b) Reactor Setup, involving the assembly of a substrate holder, reaction chamber, and precursor delivery system; (c) Introduction of Heating and Precursor, where the substrate is heated to a specified temperature and the precursor is introduced into the reactor; (d) Nucleation and Growth, where chemical processes occur as precursor molecules deposit onto the substrate, leading to the formation and growth of nanoparticles; (e) Control and Optimization, where variables such as temperature, precursor concentration, and gas flow rates are carefully controlled to regulate nanoparticle size, content, and shape; (f) In-Situ Characterization, where techniques like spectroscopy and microscopy are employed to understand nanoparticle production and growth mechanisms during the process; and (g) Post-Treatment, which involves proce-

dures like annealing, etching, or surface functionalization to improve nanoparticle quality after production.

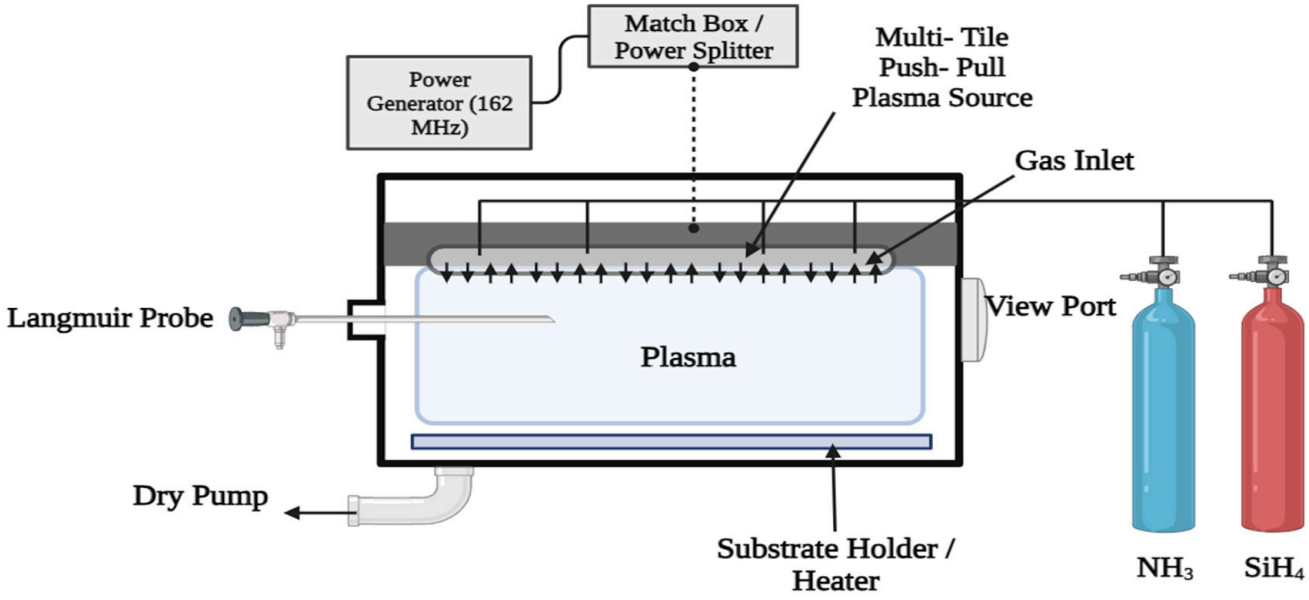

Figure 6. Plasma Enhanced Chemical Vapor Deposition used for Synthesis of Nanomaterials.

3.2.2. Sol-Gel Method

Among the plethora of synthetic methodologies employed for producing high-quality Metal Oxides Nanoparticles (MONPs) and mixed oxide composites, the sol-gel approach stands out as a widely recognized technique. This method allows for precise control over the texture and surface properties of the materials [77] (Figure 7). Variations in experimental conditions and processing parameters during the sol-gel synthesis can significantly influence the resulting material's characteristics. Thus, meticulous attention to processing variables is imperative throughout the nanoparticle synthesis to tailor the nanoparticles to specific applications [78,79]. Notably, the sol-gel method offers distinct advantages, including cost-effectiveness, homogeneity of the resultant material, lower processing temperatures, and facile production of composites and intricate nanostructures.

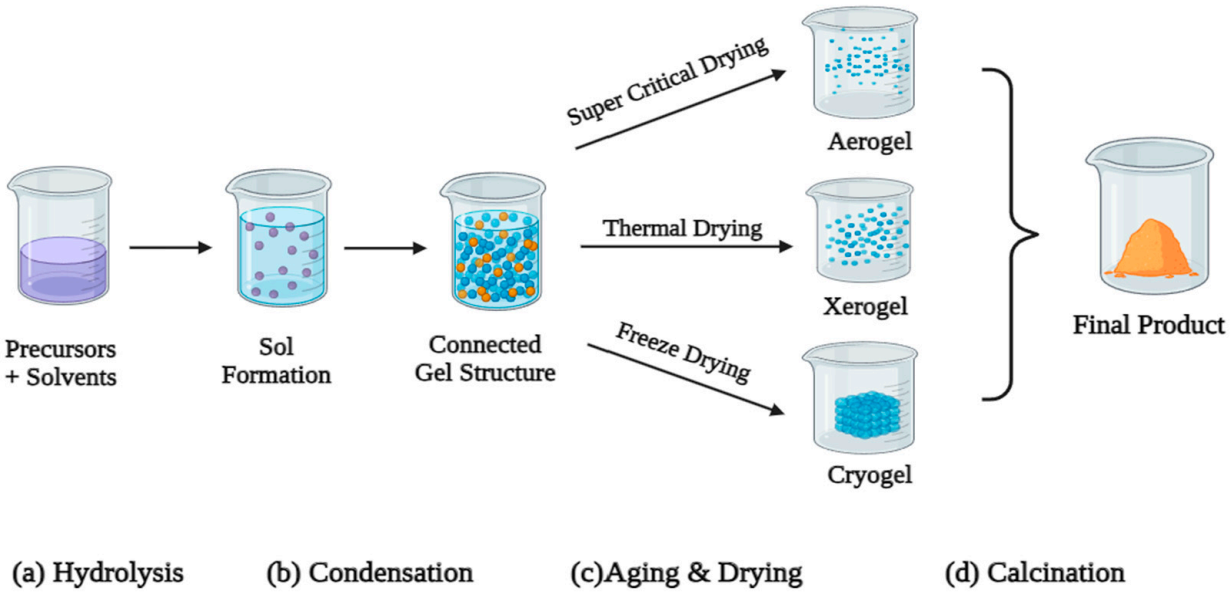

Figure 7. Application of the sol-gel process to fabricate nanoparticles [77].

The sol-gel process is a flexible and popular approach for creating nanoparticles and nanostructured compounds. A suspension of colloidal matter (sol) is created, followed by gelation to create a solid substance. The sol-gel technique has benefits, including customizable composition, control over nanoparticle size and shape, and the capacity to add different dopants or functional elements. Various nanoparticles, including metal oxides, mixed oxides, semiconductor nanoparticles, and hybrid organic-inorganic nanoparticles, may be created using the sol-gel process. It is excellent for numerous applications in catalysis, energy storage, sensors, optics, and biomedicine because it enables fine control over particle size, content, and shape. Using isopropanol as a precursor, Ristic et al. synthesized nanocrystalline ZnO powder using the following: zinc 2-ethylhexanoate, 1% ethylene glycol monomethyl ether, and tetramethylammonium($(CH_3)_4NOH$) aqueous solution [80]. According to the TEM results, the size of the NPs produced in this study varied between 20 and 50 nm. A template-assisted sol-gel method was used to create ZnO nanofibers. In a simple two-step anodization process in an oxalic acid solution, Yue et al. synthesized ZnO nanotubes with porous AAO membranes [81]. Zinc oxide nanotubes were around 70 nm in diameter and 12 nm in thickness [82].

3.2.3. Reverse Micelles Method

In this methodology, reverse micelles are formed through the interplay of at least three components, two of which are immiscible substances, while the third is a surfactant possessing amphiphilic properties [83]. This technique proves advantageous for the fabrication of nanoparticles with precise dimensions and morphology. Within this approach, reactions occur within a specialized "nanoreactor" formed by the self-assembly of surfactant molecules in the aqueous phase. The size of the resulting reverse micelles, finely tuned by the characteristics of the surfactant's polar head group and alkyl tail, ensures the preservation of both the size and shape of the produced nanoparticles [84]. Moreover, the core within the reverse micelles facilitates the controlled nucleation and growth of TiO_2 nanoparticles, providing an environment conducive to sustained development [85]. The proportions of water-to-surfactant and the solvent composition are pivotal synthesis parameters influencing the size of the reverse-micelle core. Nonetheless, adjustments to the polarity of the hydrocarbon chain and the quantity of polyoxyethylene groups offer avenues for tailoring the size and morphology of the nanoparticles [86]. Of the many available methods, the reverse micelles method, as proposed by Chandra et al., enables the production of large surface area Mo-doped TiO_2, SiO_2, and ZrO_2 NPs with concurrently evenly dispersed Mo [86]. A surfactant consisting of hydrophobic and hydrophilic regions is selected, and a compatible organic solvent (e.g., hexane and cyclohexane) that does not affect the synthesis of nanoparticles is selected. The surfactant is dissolved in the solvent under appropriate physical conditions, resulting in the self-assembly of the surfactant to form reverse micelles. A water core and a surfactant monolayer surround the water in each reverse micelle, with the hydrophilic heads pointing inward towards the water core. As more molecular precursors become available, the nanoparticles keep expanding inside the reverse micelles' water cores. By altering variables such as the precursor concentration, reverse micelle size, and reaction circumstances, it is possible to regulate the nanoparticles' size and structure. The nanoparticles are extracted by breaking the micelles, adding a non-solvent solution, or changing the physical conditions to destabilize the micellar structure. The nanoparticles are stabilized by the addition of capping agents or by dispersing them in a suitable medium (Figure 8).

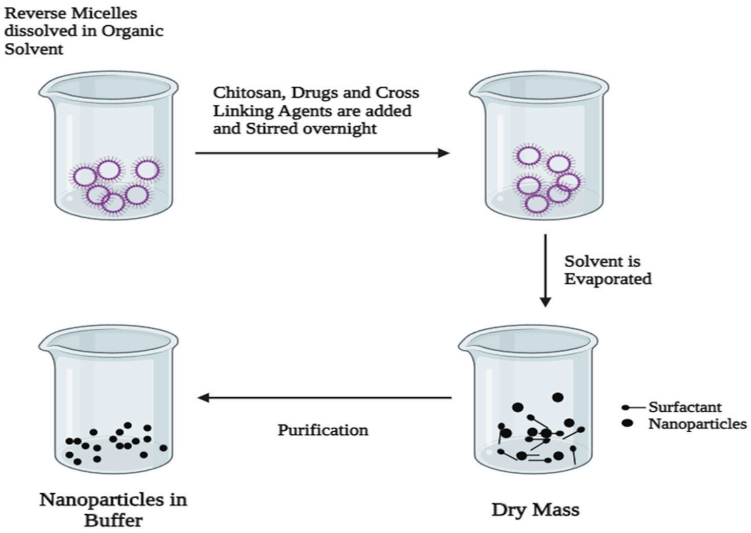

Figure 8. Reverse micelles approach in the synthesis of nanomaterials.

3.2.4. Combined Soft-Hard Templating Methods

Nanoporous materials are typically created using either a soft or hard template approach. The soft template method is one common and easy way to create nanostructured materials. The soft template method has been deemed beneficial since it is easy to execute, produces materials with various morphologies, and requires relatively mild experimental conditions [87]. Block copolymers, flexible organic molecules, anionic, cationic, and non-ionic surfactants are only a few of the soft templates used in the soft templating approach, which produces nanoporous materials [88]. Hydrogen bonding, electrostatic forces, and van der Waals forces are the most important ways the precursors and soft templates interact [89]. 3D structured mesoporous structures can be synthesized using soft templates of liquid crystalline micelles carefully structured in three dimensions.

A famous example is the production of ordered mesoporous silica solids employing alkyltrimethylammonium surfactant; these solids include lamellar (MCM-50), cubic (MCM-48), and hexagonal (MCM-41) silica. The surfactant structure, environmental parameters, precursor to surfactant ratio, surfactant concentration, and the arrangement of micelles in three dimensions are among the variables that might influence the mesoporous material structures that result from these arrangements [90]. Adjusting the surfactant carbon chain length or adding auxiliary pore-expanding agents can adjust the pore diameters of the nanoporous material. This soft template approach can be used to create a variety of nanostructured materials, including mesoporous N-doped graphene, porous aluminas, single-crystal nanorods, and mesoporous polymeric carbonaceous nanospheres [90,91] Additionally, the hard template process is often referred to as nano-casting where, to create nanostructures for specific uses, well-constructed solid materials are employed as templates and precursor molecules are inserted into the pores of the solid templates. Also, to develop mesoporous materials in the proper order, it is essential to choose the hard template. It would be ideal if these rigid templates could keep their mesoporous structure while converting precursors and remove them readily without damaging the created nanostructure. Hard templates have been made from various materials, including but not limited to wood, particles, carbon nanotubes, silica, carbon black, and colloidal crystals [92]. A synthetic pathway consists of three primary steps to create nanostructures using template techniques. The initial stage involves creating or choosing the most suitable initial template. The next step in turning the template mesopores into an inorganic solid is to fill them with a specific precursor. Mesoporous templates allow for the synthesis of a wide variety of novel nanostructured materials, including wires, rods, 3D nanostructured materials, metal oxides, and many more nanoparticles [93]. Table 1 shows the different types of conventional methods used for nanomaterial synthesis.

Table 1. Several conventional methods for the preparation of nanomaterials.

S. No	Method	Process	Materials	Technical Aspects	Results	References
1	Top-Down	Ball Milling	A. A high-energy mill B. Powder charge C. Milling medium	The kinetic energy produced by the movement of moving balls causes the chemical bonds between the molecules to break, resulting in a reduction in particle size.	A. Crystal deformation. B. Greater defect density. C. Increased material temperatures.	[1,42,94]
		Electro-Spinning	A wide range of materials.	1. High surface area-to-volume ratios, tunable surface shape, and accurate alignment. 2. Inorganic, organic, and hybrid materials, as well as core-shell and hollow polymers, have all been developed using Coaxial Electrospinning.	A. Creates continuous nanofibrous materials. B. Nanomaterials have lengths that may be expanded to many centimeters	[1,42,48]
		Lithography	A stamp containing both hydrophobic and hydrophilic areas.	1. Initially, a film is deposited onto the desired substrate to the pattern of the film. 2. After the pattern is created, the film is etched so that the designed part of the film remains, and the rest of the part is removed.	A. It can be used to design a thin layer into specified forms on a stiff substrate to manufacture electrical devices. B. The photoresist lateral shape will be transferred into the underneath layer by a subsequent treatment such as etching.	[1,42,53,95,96]
		Laser Ablation	A high intensity Laser.	1. Versatile Method. 2. Low Cost 3. Simple and Self- Standing. 4. Green Approach.	A. The system has proven its ability to function reliably under a variety of circumstances, including trials with intercontinental remote control. B. Can be used to manufacture noble metal nanomaterials from original materials. C. Pulsed laser ablation was used to create environmentally acceptable, chemical-free hybrid compositions of silver nanoparticles (AgNPs) and copper oxide nanoparticles (CuONPs) based graphene oxide (GO) nanosheets.	[1,38,42,57]
2	Bottom-Up	Chemical Vapor Deposition	Volatile matter to be turned into solid products.	1. Turns volatile precursors into a solid product that settles on surfaces. 2. Since most CVD processes are thermodynamically endothermic, the system must be provided with energy for them to react.	A. Generation of carbon nanotubes. B. Surface coatings. C. Development of chemically active radicals and ions that can take part in heterogeneous processes.	[1,40,42,73–75]

Table 1. *Cont.*

S. No	Method	Process	Materials	Technical Aspects	Results	References
		Sol-Gel Method	A. Metal Alkoxides B. Titanium IV Isopropoxide. C. Zinc-Acetate dehydrates oxalic acid and ethanol. D. Tin-chloride pentahydrate and Ammonia solution.	1. The precursors, such as metal alkoxides, are hydrolyzed in water or alcohols. 2. Condensation of nearby molecules results in the removal of water and alcohol, the formation of metal oxide linkages, and the growth of polymeric networks to colloidal dimensions while they are in the liquid state. 3. The structure and characteristics of the gel continuously change as a result of the aging process. 4. It is a very economically friendly method used to synthesize nanoparticles.	Synthesis of TiO_2, ZnO, SnO_2, CaO Nanoparticles.	[42,76,78,79,97,98]
		Reverse Micelles Method	There are at least three components, two of which are immiscible and the other a surfactant with amphi-phallic qualities.	1. Synthesizes nanoparticles using a minimum of 3 components. 2. A nanoreactor is created by self-assembling molecules in the water phase. 3. The size of the resulting reverse micelles enables controlling the size and shape of the NPs formed. 4. The water-to-surfactant proportion and the composition of the solvent medium are the fundamental synthesis factors that affect the size of the reverse-micelle core. 5. By modifying the polarity of the hydrocarbon chain and the amount of polyoxyethylene groups, the size and form of the NPs may be adjusted.	A. Nanoparticles with a particular size and structure. B. This approach also enables the production of large surface area Mo-doped TiO_2, SiO_2, and ZrO_2 NPs.	[42,83–96,99]
		Microfluidic Approach	Typical substances include ceramics, glass, silicon, metals, and polymers.	1. Distinctive structure allows smaller reagent volume. 2. Precise control of mixing of fluids. 3. Efficient transport of mass. 4. Better heat transfer. 5. Eased automation. 6. Lesser reaction time.	Development, manufacture, and use of disposable, portable, and economical equipment.	[9,41,42,100]

3.2.5. Microfluidics

This field studies and develops devices for processing or manipulating fluids in extremely minute volumes (10^{-9} to 10^{-18} L) through channels with dimensions ranging from 10 to 100 μm [9]. The dimensions and exclusive geometries of microfluidic devices enable lesser reagent volume use, ease of automation, successful mass transport, better heat transfer, precise control of fluid mixing, and lesser reaction time. The benefits of microfluidic approaches over generally known methods led to the design, fabrication, and usage of portable, low-cost, and disposable devices [41,100]. Microfluidics emerged by amalgamation of domains like biology, fluid mechanics, physics, chemistry, and electronics [9,29]. Although microfluidics is a relatively newer concept, micro-channels have been used earlier in some equipment like electrophoresis and flow reactors as capillaries and gas chromatography [101]. As time passed, better and more sophisticated equipment requiring liquid flow through microchannels was documented in literature and patents [12]. In the 1990s, the growth in microfluidics technologies was recognized and became an essential tool with gigantic potential applications [15,16,102]. Various operations like separation processes, reaction engineering, reactor design, compound detection, etc., employed small or miniature microscale instruments [13,29]. Much research has also been done based on different applications and characteristics of microfluidic devices. Some of their applications include lab-on-a-chip or organ-on-a-chip microreactors. Based on their use, there are various fabrication methods for these devices [103,104]. Due to different reports in the literature on different techniques and fabrication methods of microfluidic devices [105], it has been well understood that the potential of microfluidic applications is gigantic in academics and industries [104]. Moreover, several day-to-day applications of microfluidic devices have also been reported in the literature, such as HIV testing, covid testing, hepatitis A, B, and C testing, in-home pregnancy testing, and herpes testing [106,107]. This paper aims to thoroughly describe microfluidic technologies and their applications in nanomaterials production.

A number of the major drawbacks of conventional synthesis methods can be circumvented using microfluidic technology, thanks to the small capillary width and the high surface-to-volume ratio that results. Synthesis and engineering of nanoparticles for medication administration have been its primary drawbacks. Nanomaterials loaded with drugs made utilizing microfluidic processes have the potential to outperform their conventional bench counterparts in terms of blood circulation times, formulation yield, and monodispersity [100]. Microfluidics is a modern approach to regulating fluids in microscale channels, and this has found a huge number of applications in the isolation and detection of cells [108], easing the analysis of biological cells and vesicles [46], and point-of-care testing [109]. The advancing state of microfabrication technology encourages the insertion of numerous structures into the device, making it possible for various processes to be carried out continuously, sequentially, and automatically. Additionally, the improved mixing provided by microfluidic devices results in the production of homogeneous and compact nanoparticles. The average size of lipid nanoparticles produced by microfluidics is 20 nm; utilizing the same chemicals and traditional mixing techniques, this diameter rises to 70 nm [110]. Microfluidic technologies enable simple control of nanoparticle parameters. Microfluidic devices can create nanoparticles of various sizes, shapes, structures, rigidities, and surface modifications with high reproducibility. The microfluidic approach can produce nanoparticles at up to 3.15 kg per day by paralleling microchannels, increasing the flow rate, and establishing novel manufacturing paradigms [111,112]. Nanomaterials' size, shape, stiffness, surface charge, and surface component largely determine their colloidal stability, circulatory half-life, systemic toxicity, cellular absorption, bio-distribution, and targeting capabilities [113]. The different microfluidic approaches to control nanomaterials' physical and chemical properties have been discussed below.

Size

Kimura et al. and Thiermann et al. investigated the molecular assembly process using a microfluidic approach for nanomaterial development [114,115]. They found that the size of aggregates is primarily influenced by nucleation time and growth time. Factors such as flow rate, Reynolds number, and relative flow rates of oil and water phases govern fluid mixing, affecting growth time. Additionally, precursor concentration impacts nucleation time. Mijajlovic et al. studied the modification of 1-palmitoyl-2-oleoyl-sn-glycero-3-phosphocholine (POPC) vesicle size (60 to 170 nm) by regulating fluid flow ratio and POPC concentration in a microfluidic device [116]. Microbubbles were utilized by Gunduz et al. to create ethyl-cellulose nanoparticles with diameters varying from 10 to 800 nm using a microfluidic V-junction device [117]. Nanoparticles made of poly(lactic-co-glycolic acid)-polyethylene glycol (PLGA-PEG), polystyrene, lipid vesicles, and iron oxide shrank considerably when the Reynolds number was raised from 500 to 3500. According to this research, microfluidic techniques make anticipating and screening for optimal experimental settings easier [118].

Shape and Structure

He and Park stated that nanoparticle shape and structure are crucial in cellular absorption and drug loading. Polymeric nanoparticles can also have their pore size and degree of compactness altered using microfluidic procedures [119]. The study found that the tightness of the polymer nanoparticles made using hydrophobically enhanced chitosan could be regulated by adjusting the TFR, FRR, and hydrophobic characteristics of the chitosan chains [120]. Mesoporous silica nanoparticles with different aspect ratios were synthesized in a microchannel with a spiral form. The structure of the mesoporous silica products changed significantly when the circulation rate and reactant concentration were adjusted. They ranged from spherical nanoparticles to nanofibers with a mean size of 40 nm [99]. Furthermore, nanoparticles' interior structures can be controlled using microfluidics. A nano-in-nano vector was created by integrating the drug nanocrystal cores into a polymer shell employing a microfluidic device [30]. These nanoreactors increased stability, biodegradability, pH responsiveness, and extremely effective drug loading.

Rigidity

The rigidity of nanomaterials as drug carriers significantly impacts the blood circulation, cellular absorption, tumor buildup, and tumor penetration of nanoparticles [121]. Microfluidic techniques have enabled the fabrication of nanoparticles with adjustable stiffness, allowing for a detailed exploration of how rigidity influences drug delivery. By precisely controlling fluid flow through microchannels, researchers have delved into the lipid layer structure and studied the anticancer effects of nanomedicines with varying stiffness levels. In a recent study, the efficacy of stiff nanocarriers in delivering drugs to tumors was investigated in vivo. The results demonstrated that stiff nanocarriers significantly enhanced tumor accumulation and exhibited a therapeutic impact. A pH-sensitive nanocomplex was also developed to address drug-resistant malignancies [113]. This nanocomplex comprised a PLGA core and a pH-sensitive co-polymer shell, both synthesized within a microfluidic device for precise control and enhanced efficacy. The doxorubicin-loaded nanoparticles dramatically improved tumor treatment effectiveness by increasing cellular absorption and lysosome escape [122].

Surface Modification

Targeted medication delivery can be made more efficient and effective via surface modification. Nucleic acid-based medicines are better entrapped when cationic lipids are modified. For instance, in a microfluidic system, Di Santo et al. treated nanosized graphene oxide flakes by using the cationic lipid DOTAP (1,2-dioleoyl-3-tri-methylammonium-propane), thus overcoming the problem of binding double-stranded DNA onto graphene oxide-based nanomaterials [123]. Thanks to this fresh strategy, a risk-free and highly effective nanocar-

rier for carrying genes was created. Modifying targeting ligands can boost cellular tumor absorption and accumulation to improve tailored cancer treatment. Furthermore, it has been demonstrated that the chemical makeup of the nanocarrier on the surface affects the surface charge of the nanocarrier in physiological settings [100].

4. Microfluidics Methods of Preparation of Nanomaterials

The high surface-to-volume ratio and small capillary size are two of the main problems with conventional synthesis methods; however, these issues can be addressed with an understanding of microfluidics. The characteristics of synthesized nanomaterials may be precisely controlled in microfluidic processes thanks to these traits, which enable quick and uniform mass transfer. By precisely adjusting the volumetric flow rate of the fluid and the dimensions and geometry of the microfluidic platform, microfluidic synthesis can generate monodisperse nanoparticles that are more uniform in size and shape than those produced by bulk techniques, and they also have better agglomeration efficiency [124]. Microfluidic devices are included in the sample preparation, reaction, separation, and detection scope, which function using fluid flow within microscale channels and chambers of predetermined dimensions [29]. The microfluidics approach permits uniform and fast mass transport and provides enhanced control over the properties of the nanomaterials produced [41]. Regarding synthesis methods, the pattern handling determines which reactor (or microreactor) is used: single-phase flow or multi-phase flow. The following are descriptions of these methods: when looking at different approaches to synthesis, the two most common kinds of microreactors that manipulate flow patterns are those that use one phase (droplet-based microfluidics) or many phases (continuous-flow microfluidics) [18,125].

4.1. Single-Phase Flow Systems

Single-phase approaches are primarily employed in the manufacture of nanoparticles inside microfluidic devices. This flow model is the alternative of preference in many works because of its ease, homogeneity, and adaptability in calculating process variables, like volumetric flow rate, amount of reagent, time required for reaction, and temperature. In general, single-phase synthesis is accomplished under laminar flow with a Reynolds number of less than 10, dominated by molecular interdiffusion due to the absence of turbulence [16,17]. Rare occurrences of convection events and significant occurrences of lateral diffusion are observed when single-phase steady-flow for the microfluidic method is established. In a single-phased (continuous-flow) system, fluids are combined by diffusion in laminar flow streams using one or more solvents during the fabrication of nanoparticles. Diffusion is the progressive mixing of materials caused by molecules moving by Brownian motion from a location of higher concentration to one of lower concentration. Mathematically, diffusion is explained by Fick's law [126] as follows:

$$j = -D\frac{d\varphi}{dx} \tag{1}$$

where, D is the diffusion coefficient (m^2/s), j is the diffusive flux (mol/m^2 s), φ is the species concentration (mol/m^3), and x is the position of the species (m).

In microfluidic channels, the physical features of fluid flow are described by the Reynolds number (Re). The following formula can be used to determine the relationship between inertial and viscous forces using the Re [127]:

$$Re = \frac{inertiaforce}{viscousforce} = \frac{\rho vD}{\mu} \tag{2}$$

where dynamic viscosity (kg/m·s) and kinematic viscosity (m^2/s) are represented by μ and μ/ρ, channel length (m) represented by D, average flow velocity (m/s) by v, and fluid density (kg/m^3) by ρ. The Reynolds number is usually kept below 100 [128]. Hence, continuous-flow microfluidics are generally preferred when controlling parameters, repro-

ducing the results, and homogeneous product characteristics [8]. The environment in the single-phase flow systems is best suited for synthesizing small nanoparticles with a small range of size distribution of particles (especially used in pharmaceutical companies) [125].

Micromixers for single-phase microfluidic flow systems fall into active and passive categories. In the active micromixer, the mixing process is driven by electric, pressure, acoustic, magnetic, and thermal fields to achieve better mixing [129]. An acoustic-driven micromixer was introduced with integrated sharp edges and bubbles in its channel to improve the mixing speed and homogeneity of the produced polymeric nanoparticles [130]. On the other hand, the passive type of micromixer's mixing mechanism is driven by the channels' architecture. Passive micromixers have been designed and developed over the years with a wide range of novel architectures, such as multi- and parallel laminations, obstacle-channel designs, curved channel topologies, serpentine patterns, herringbone structures, unsymmetrical geometries, etc. A gear-shaped micromixer has been employed to synthesize silica nanoparticles [131]. Further, two main types of micromixers have been reported so far in the basics of continuous-flow microfluidic design: Y-shaped and T-shaped (Figure 9). For single-phase flow nanoparticle synthesis, Y-shaped microfluidic systems are further categorized into two-way or three-way channels based on the flow type [129].

Singh et al. reported successfully doped Mn in a ZnS semiconductor using 1-thioglycerol solvent at room temperature and 80 °C in a T-shaped micromixer [132]. The zinc-blende structure of Mn-doped ZnS nanoparticles was demonstrated by x-ray diffraction analysis and transmission electron microscopy, which revealed an average particle size of about 3.0 nm. Chen et al. efficaciously synthesized mesoporous silica MCM-41 using ethanol, CTAB, NH_4OH, 3-aminopropyltrimethoxysilane (APTMS), and NH_4NO_3 as solvents and additives. A T-shaped micromixer was used to get a particle size of 400 nm at 25 °C [133]. In another study, the T-shaped microreactor-assisted nanoparticle deposition (MAND) process was used to synthesize the nanostructured ZnO as an anti-reflective coating on a textured silicon. NaOH, isopropyl alcohol (IPA), Zn $(COOCH_3)_2.2H_2O$, and CH_3COONH_4 were used as solvents and additives for the process [134]. Sodium hydroxide, ascorbic acid, and copper chloride formed a precipitation process that could be easily controlled to produce cubic cuprous oxide (Cu_2O) nanoparticles in a T-shaped micro-mixer. The results showed that the size distribution of Cu_2O particles shrank, and their particle size reduced as the concentration of ascorbic acid, feed flow rate, sodium hydroxide, and temperature rose [135]. Chang et al. used magnetic stirring of Fe_3O_4 nanomaterial to mediate active mixing in T-shaped micromixers, circumventing the ineffectiveness of passively transferring two solutes (blue phenol dye and citric acid) [136]. A ferric oxide magnetic nanoparticles and citric acid solution were prepared to create nano- or micro-rods that could spin in lockstep with a magnetic field applied from outside. When the magnetic materials were spun at a speed of 10.47 rad s1 and contained 0.05 weight percent, efficient mixing was accomplished with a driving force of 6.6 mT.

A Y-shape micromixer synthesized silver nanoparticles using silver nitrate ($AgNO_3$) and sodium borohydride ($NaBH_4$). A microreactor operating at 1 mL/min (0.001 M) for $AgNO_3$ and 3 mL/min (0.003 M) for $NaBH_4$ demonstrates an optimal particle size of 4.8 nm. According to residence time distribution (RTD) statistics, the Pe_{ax} number peaked at 0.39 at *Re* number 67 (flow rate of 7 mL/min), indicating less axial dispersion. Comparison analysis between batch and microreactor processes, and additional SDS and CTAB effects were also conducted. Since cationic CTAB has a positive charge on its head, it causes aggregation, which causes the particle size to grow as the CTAB loading increases. SDS encourages decreasing silver nanoparticle size [137]. Song et al. synthesized Cu nanoparticles using a tubular microfluidic reactor through a controlled growth process using tetrahydrofuran, lithium hydrotriethyl borate, 3-[N,Ndimethyldodecyl- ammonium]- propane- sulfonate, acetone, and ethanol as solvents and additives [138]. In a Y-mixer, the preformed NP seed solution and the washing reagent were continuously mixed to allow for the controlled release of the surfactant surrounding the small NP seeds. Using this controlled-growth approach in the micro-tubing, nearly monodispersed copper NPs with a critical size of 135.6

± 11.4 nm could be produced [139]. In another study, a double-layer Y-shaped splitting and recombination (SAR) micromixer was promoted to produce silver nanoparticles in a controlled manner. The microchannel of the micromixer was shaped like a double-layer Y, which caused the two-phase fluid to split and recombine, expanded the area of contact between the fluids, enhanced the mixing effect of $AgNO_3$ and $C_6H_{12}O_6$, and expedited the phases of silver atom precipitation and nucleation [139]. Lately, green synthesis of AgNPs using a traditional medicinal plant *Ipomea quamoclit* L., was carried out using a microfluidics-based Y-shaped serpentine micromixer. According to the Dynamic Light Scattering study, the nanoparticle's diameter was around 72 nm. The antibacterial activity of the nanoparticles was evaluated in several fungi and bacteria, including *Aspergillus niger*, *Candida albicans*, *Enterobacter faecalis*, *Staphylococcus aureus*, and *Micrococcus luteus* [140].

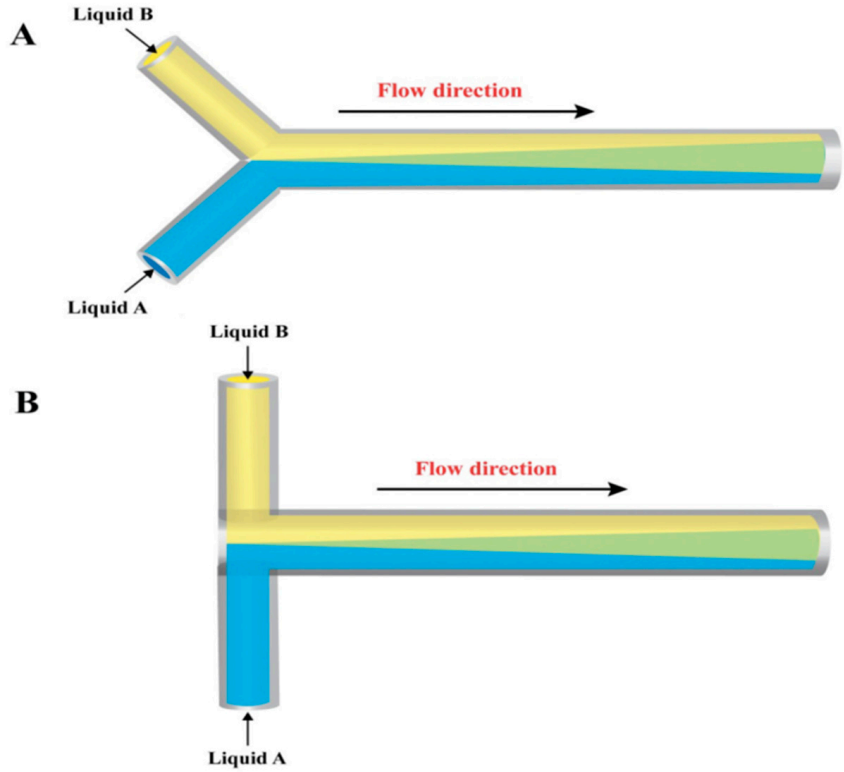

Figure 9. Y- and T-shaped micromixers: (**A**) Y-shaped and (**B**) T-shaped [141,142].

Various obstacles in different shapes (triangle, ellipse, circle, and diamond) have been incorporated within the T micromixers to improve the mixing efficiency and shorten the mixing duration. Using numerical simulations, it was found that the diamond-shaped obstacles performed better than others [143]. In addition to Y-type and T-type varieties (Figure 9), other contemporary passive micromixers for nanoparticle production have been reported by several authors, which have enhanced efficiency, reduced cost, simpler manufacture, and faster mixing [141]. Niculescu et al. recently reported a novel device that uses vortex mixing principles and 3D microfluidic platforms to create core-shell nanoparticles, providing a more effective substitute for traditional microchips and synthesis techniques [144]. The ability to rapidly produce homogenous salicylic acid-functionalized iron oxide (Fe_3O_4-SA) nanoparticles has shown the versatility and efficiency of the 3D vortex-type multilayered microreactor platform for micromixing. A novel passive micromixer design, utilizing a wet etching process, was developed recently by utilizing helical-shaped stainless steel AISI-304 inserts. The insert's presence increased the degree of mixing by passively creating high shear stress and diffusive advection. Achieving nanoparticles with a mean size of 130 nm and a PDI as low as 0.05 may be possible, with the insert facilitating an effective mixing of immiscible streams during residence periods

less than 130 ms. Jahangir et al. developed a novel customized microfluidic chip (MF) with omega-shaped microfluidic micromixers, which was fabricated on a silicon wafer (used as a master) by the photolithography for the synthesis of ultrasmall silver nanoparticles [145]. In contrast to traditional benchtop-assisted NP synthesis, this work revealed the important role of the microfluidic approach in the one-step, environmentally benign synthesis of ultrasmall and homogenous nanoparticles utilizing a solvent of choice. Guo et al. developed a unique passive micromixer that efficiently mixes many solutions using an elementary spatial Tesla valve design [146]. The Tesla valve micromixer offers many benefits when combining biological and chemical interactions to generate chitosan nanoparticles. Hong et al. developed a new passive micromixing technique that combines the instability created by curved streamlines in a "gear-shaped" microchannel with the synergistic effects of inertia-elastic flow instability in side-wells [131]. They used the unique mixing method to continuously produce silica nanoparticles with a more uniform size distribution and regular shape than those in a Newtonian fluid. Kimura et al. developed an invasive lipid nanoparticle production system (iLiNP) that produced 80 nm-sized lipid nanoparticles (LNPs) with encapsulated small interfering RNA (siRNA) [114]. These LNPs functioned as nano-drug delivery system carriers in an in vivo experiment with favorable outcomes. The synthesis of Ni nanoparticles with an average size of around 80 nm was reported by Zeng et al. using a caterpillar-type micromixer. Ethanol, NaOH, N-cetyl N,N,N,trimethyl ammonium bromide (CTAB), and PVP have all been employed as additives and solvents. When hydrogenating p-nitrophenol to p-aminophenol, the produced nickel nanoparticles outperform the commercially available Raney Ni catalyst in terms of catalytic activity [147]. In the fabrication of silica nanoparticles, a simple micromixer with short mixing-length baffles can provide efficient mixing over a broad range of flow rates. A moderate flow rate of 0.1 mL/h would result in a 250 $\pm$ 50 nm average particle diameter. The advantages of this micromixer are its short obstacle channel, ease of design, and low number of mixing units [148].

4.2. Multi-Phase Flow (Droplet-Based) Systems

Unlike single-phase microfluidics, the multi-phase flow (or segmented flow) is used when more than one immiscible liquid is involved [16]. Passive mixing is facilitated in such systems (heterogeneous) by improving the rate of mass transfer, decreasing the residence time, and mitigating the reagent or product deposition inside the channels and walls [8]. In general, there are two basic categories into which microfluidic methods to create droplets or bubbles can be divided: the surface method and channel-based microfluidics [99] The channel-based approach involves the interaction of dispersed and continuous phases to produce single droplets or bubbles. On the other hand, the breakage happens in the planner surface technique, also known as digital microfluidics, from an actuation mechanism by electrowetting or dielectrophoretic approaches. Within the category of channel-based microfluidics, some common geometries for creating droplets or bubbles in microfluidic systems are T-junction, flow focusing, co-flowing, membrane, and step emulsification (Figure 10) [149].

Within microfluidic systems, T-junctions are a typical subclass of cross-flowing junctions widely used for generating immiscible fluid segments [150]. Flow-focusing geometry is used for the production of dispersed phase droplets, and it is subcategorized into dripping flow for the lower flow rate of fluid and jet flow for the high dispersed phase flow rate of fluid [151]. Furthermore, co-flowing geometry has been primarily developed to generate monodispersed droplets/bubbles. The droplet generation in the co-flowing geometry in the dripping and jetting regime is similar to flow-focusing geometry and commonly described by Rayleigh–Plateau instability theory [152]. Generally, polymer/metal/ceramic-made membranes are produced to flow many droplets uniformly [153]. Step emulsification is advantageous as it produces a high monodispersity because of the impact of flow rate or variations in pressure. Nisisako and Torii developed parallel droplet formation microchannels in addition to these popular types to produce monodispersed droplets in large

quantities [154]. A straight-through geometry employing an array of uniform through-holes is one example of these structures [155].

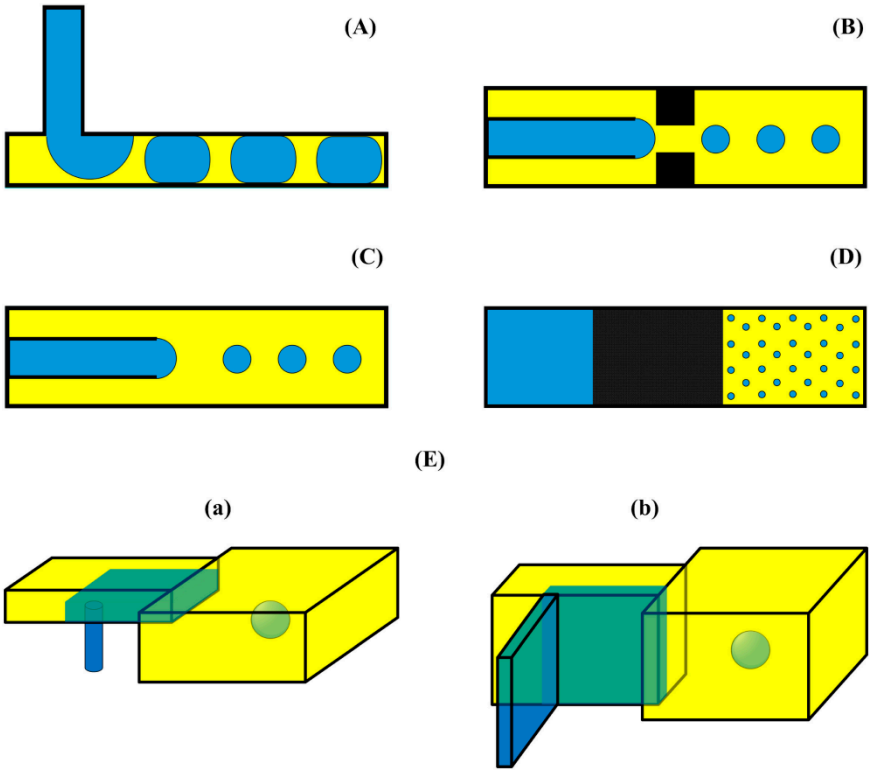

Figure 10. Operating mechanisms and shapes for droplet or bubble production in microfluidic devices: (**A**) T-junction, (**B**) flow-focusing, (**C**) co-flowing, (**D**) membrane, and (**E**) step emulsification ((a) vertical step. (b) horizontal step) [149].

As the name shows, droplet-based microfluidics relates to developing and managing distinct globules within microchannels [156]. Globule creation is synchronized throughout device dimensions, channel geometry, and volumetric or mass flow rate of every liquid, permitting accurate checking and control of the fabrication process [157]. That being said, several multi-phase flow scheme limitations must be considered while scheming this applicability. One of the downsides is the reduced constancy of the globules. This may be improved by adding surfactants; however, this treatment is inappropriate for all conditions. One more concern is that droplets are not entirely inaccessible, as a degree of material swap between globules and droplets occurs [157]. Nevertheless, whether these downsides affect the preferred product depends on the device's application. Table 2 shows the different types of microfluidic devices used for inorganic and organic nanomaterial synthesis [41].

Table 2. Summary of inorganic and organic nanomaterials synthesized using microfluidic devices [Adapted from [41]].

Fabrication of Nanomaterials	Type of Micro-Size Reactor	Utilization of Chemicals	Fabrication Conditions	Morphology	References
Inorganic nanoparticles					
AuNPs	Polydimethylsiloxane microreactor	$NaBH_4$ for reduction, $Na_3C_6H_5O_7$ for capping and $HAuCl_4$	Operating time of 5 min at ambient temperature	~2 nm of particle size	[158]
AuNPs	Polydimethylsiloxane microchannel	Utilization of $HAuCl_4$ and $NaBH_4$ for gold seeds, $AgNO_3$, ascorbic acid	Proper stirring followed by a controlled flow rate	Desired morphology of Au-nano-bipyramids	[159]
AgNPs	Flash fabrication in the spinning disc process	$AgNO_3$, ascorbic acid, starch, and polymers (polyethylene glycol (PEG) and poly(4-vinyl pyridine))	Vigorous stirring forms a thin film of fluid at ambient temperature on a rotating disc	Particle size is controlled by disc speed	[160]
AgNPs	Polydimethylsiloxane device with small volume (micro to femto liter) of reaction mixture	$AGNO_3$, $Na_3C_6H_5O_7$, tannic acid, mineral oil, PDMS	Vigorous mixing, fast reaction, colloid formation at ambient temperature	Controlled particle size uniformity and polydispersity in droplet PDMS chip	[161]
AgNPs	Polydimethylsiloxane microchip with droplet seed formation	$AgNO_3$ and $NaBH_4$ used to fabricate Ag-seeds, $Na_3C_6H_5O_7$, molten paraffin	Microdroplets in microreactor at 60 °C for seed formation	Particle size is controlled by adjusting temperature, time, and Ag^+ ion concentration	[162]
ZnO NPs	Used flow-through equipment and microreactor under hydrothermal fabrication	$ZnSO_4$ (0.001 mol/kg) and KOH (0.004 mol/kg) solutions	Hydrothermal fabrication at 400 °C in a furnace followed by crystal separation and drying at 60 °C	Achieved particle diameter of 9 nm	[163]
ZnO nanostructures	Microfluidic chip with multifunctional properties	$Zn(CH_3COO)_2{\cdot}2H_2O$, $HN(CH_2CH_2OH)_2$, $ZnNO_3{\cdot}6H_2O$, $C_6H_{12}N_4$, 28% v/v, NH_3 solution	Dip-coating and annealing to fabricate ZnO seed followed by mixing with other reagents and vigorous mixing at 60 °C for 20 min	Growth of microstructure ZnO of different morphology at channel wall of capillary tubes	[164]
TiO_2 NPs	Microchannel reactor made up of ceramic material and glass cover	Two solution, titanium(IV) isopropoxide (TTIP) in 1-Hexanol and formamide (CH_3NO) in H_2O	Reacted at the interface of two insoluble currents (TTIP and CH_3NO) in microchannel	Controlled particles of 10 nm of anatase morphology formed	[165]
SiO_2 nanofibers	Microfluidic process in polydimethylsiloxane reactor (spiral-shaped)	Cetyltrimethylammonium Br (CTAB), NH_3 solution, tetraethyl orthosilicate (TEOS), ethyl alcohol	CTAB in NH_3 solution and TEOS solution mixed from two in-lets and react to form SiO_2 nanofiber at ambient temperature	Fabricated mesoporous SiO_2 nanofiber; Morphology control by controlling the flow rates of two solutions or reagent concentration	[166]
Spongy, porous, and spherical SiO_2 NPs	Spiral PDMS microreactor laminar flow	CTAB, NH_3 solution, TEOS, 1,3,5-trimethylbenzene (TMC)	Vigorous mixing of two solutions (CTAB in NH3 solution and TMC in TEOS) to react and form NPs	Fabricated spherical and porous SiO_2 NPs with an average diameter of 1200 nm	[167]

Table 2. *Cont.*

Fabrication of Nanomaterials	Type of Micro-Size Reactor	Utilization of Chemicals	Fabrication Conditions	Morphology	References
Cobalt NPs	Microfluidic reactor	$CoCl_2$, tetrahydrofuran (THF), $LiBH(C_2H_5)_3$, stabilizer 3-dimethylammonio -1-propanesulfonate	Fabricated in the microfluidic reactor with fine tuning of quenching time and flow rates of reactants (0.08 to 0.9 mL/min)	Obtained crystals of CoNPs	[168]
Fe_2O_3 NPs	Spiral-shaped Cu wire microreactor with continuous flow	$Fe(NO_3)_3{\cdot}9H_2O$, NaOH, CTAB	The flow of NaOH and $Fe(NO_3)_3{\cdot}9H_2O$ through a syringe in a spiral microreactor to co-precipitate and reduce at ambient temperature	Obtained 6 nm of particle size at 1 mL/min flow rate of reactants	[169]
CdSe quantum dots (QDs)	Polytetrafluoroethylene microreactor	CdO, Se, diphenyl ether, trioctylphosphine-oleic acid (TOP-OA), $CHCl_3$	Solution mixture of CdO, OA, and diphenyl ether heated at 180 °C and Se TOP prepared by ultrasonication; both solutions reacted to form CdSe QDs	Obtained photoluminescence CdSe QDs	[170]
Sulfur NPs	Y- and T-type microfluidic reactors	Dry sulfur (sublimed), CTAB, solvent and anti-solvent as CS_2, and ethanol	Solvent (sulfur and CS2) and anti-solvent (CTAB in ethanol) mixed to precipitate and obtain suspension; Spray dry to synthesize sulfur NPs	Obtained 15–50 nm particle size	[171]
Organic nanoparticles					
Liposomes	Microreactor made up of thermoplastic with microfluidic vertical flow and hydrodynamic focusing (VFF and MHF system)	Lipid of 80 mmol/L, solvents	Size controlled by flow rate ration, i.e., aqueous/ lipid-solvent flow	Obtained 80–200 nm of size of monodispersed vesicles	[172]
Liposomes	Reactor with V-shaped off-the-shelf Teflon tubing	Ethanol and different types of lipids (1,2-distearoyl-synglycero-3-phosphocholine, N-carbonylmethoxypolyethyleneglycol 2000)-1,2-distearoylsn-glycerol-3-phosphoethanolamine, Cholesterol)	The reaction of aqueous and ethanol solution of lipids with controlling flow rates at 25 °C	Obtained 50–70 nm of diameter particle size	[173]

Table 2. *Cont.*

Fabrication of Nanomaterials	Type of Micro-Size Reactor	Utilization of Chemicals	Fabrication Conditions	Morphology	References
Liposomes	Used ultrasonication with microfluidic devices	Phosphatidylcholine from egg and cholesterol	Microfluidic devices placed in a sonicator with controlled flow rates for microdispersion	Obtained 66.27 to 189.9 nm of particle size depending upon the flow rates	[174]
Polylactic-co-glycolic acid (PLGA) NPs	Computational fluid dynamic-based micromixing in the microfluidic system made up of Teflon material (plus-shaped chip)	Dimethylsulfoxide (DMSO) to dissolve PLGA and aqueous polyvinyl alcohol (PVA) solution	The reaction of PLGA dissolved in DMSO with aqueous PVA for nanoprecipitation in the microdevice	Obtained uniform and harmonious spherical particle size (238 nm)	[175]
Polyethylene glycol (PEG)-PLGA NPs	Microreactor of polyimide film with three-dimensional flow	CH_3CN dissolved polymers (PEG and PLGA) and H_2O	The flash flow of 11 milli second in a unit microchannel of reaction mixture	Obtained 50–85 nm of particle size	[176]
Polycaprolactone (PCL) NPs	Microfluidic chip made up of glass; different channel dimensions and confluence angles (CA)	PCL dissolved in THF (organic phase); H_2O, PVA, and surfactants (tween-80) (aqueous phase) Aqueous phase: PVA, Tween 80, Milli-Q Water, Organic phase: PCL, THF	Flow rate, ratio, channel width, and its length, and CA of inlet channel affected particle size, distribution, and polydispersity index; Non-solvent precipitation	Obtained 40–370 nm of particle size NPs	[177]
Hyaluronic acid (HA) NPs	T-shaped microchannel device made up of glass	Ethanol, isopropyl alcohol, acetone (organic phase); Na-HA, H_2O, EDCI, ADH (aqueous phase)	Synthesized HA NPs at a pH of 6.0 at the interface of organic and aqueous phases inside the microchannel	Obtained homogeneous 140–460 nm of particle-sized	[178]

5. Conclusions

Nanomaterials can adopt a wide range of different shapes and chemical compositions through various chemical processes. Their adaptability makes it possible to tailor their design, size, surface changes, solubility, deformability, charge, and other qualities to meet the needs of various applications. Unfortunately, the reaction conditions that affect the end product are not always completely and precisely controlled using traditional nanomaterial synthesis methods. Microfluidic devices, an emerging technology that provides a controlled environment for synthesizing high-quality nanoparticles, have solved this challenge. Nanoparticles, drug-carrier systems, APIs, composite nanomaterials, and cells can all be made using these instruments that precisely manipulate tiny quantities. Since it guarantees consistency in the size of particles and content, this manufacturing technology has many benefits, including improved performance in a wide range of applications. The potential for further advancements and research in this field is substantial. The technology of microfluidic devices holds the promise of continued refinement, leading to more efficient and cost-effective methods of producing a wide range of nanomaterials. As our understanding of nanotechnology continues to evolve, so will our ability to harness its potential for various practical uses in our daily lives. The ongoing investigations into the capabilities of microfluidic devices and their applications in nanomaterial synthesis will undoubtedly yield even more exciting discoveries and innovations in the near future.

Author Contributions: Conceptualization, S.R., R.K., A.A., S.R. and S.C. (Sankha Chakrabortty); methodology, S.B., R.K., A.A., B.-H.J., A.C., J.N., A.B., S.B., S.K.T. and S.C. (Snehagni Roy); investigation, S.K.T., S.B., A.B., B.-H.J., J.N. and S.C. (Snehagni Roy); writing—original draft, S.R., R.K., A.A., S.R., A.C. and S.C. (Sankha Chakrabortty); writing—review and editing, S.K.T., B.-H.J., S.B., S.C. (Sankha Chakrabortty), A.B. and J.N.; supervision, R.K., S.K.T.; funding acquisition, B.-H.J. and S.C. (Sankha Chakrabortty). All authors have read and agreed to the published version of the manuscript.

Funding: This work was supported by the National Research Foundation of Korea (NRF) grant funded by the Korean government (MSIT) (No. RS-2023-00219983). S. Chakrabortty acknowledges the University Grants Commission, Government of India, under the UGC-FRPS scheme (Project No. F.30-575/2021).

Data Availability Statement: No new data were created or analyzed in this study.

Conflicts of Interest: The authors declare no conflicts of interest.

References

1. Iqbal, P.; Preece, J.A.; Mendes, P.M. Nanotechnology: The "top-down" and "bottom-up" approaches. In *Supramolecular Chemistry: From Molecules to Nanomaterials*; John Wiley & Sons, Ltd.: Hoboken, NJ, USA, 2012.
2. Yusuf, M.; Kumar, R.; Ali Khan, M.; Ahmed, M.J.; Otero, M.; Muthu Prabhu, S.; Son, M.; Hwang, J.H.; Hyoung Lee, W.; Jeon, B.H. Metal-organic framework-based composites for biogas and natural gas uptake: An overview of adsorption and storage mechanisms of gaseous fuels. *Chem. Eng. J.* **2023**, 478. [CrossRef]
3. Alhamad, A.A.; Zeghoud, S.; Amor, I.B.; Zaater, A.; Amor, A.B.; Aouadif, A.; Hemmami, A. A short review of nanomaterials: Synthesis methods, properties, and applications. *Algerian J. Chem. Eng.* **2023**, *1*, 1–7.
4. Singh, S.S.; Jena, B.; Roy, S.; Nayak, S.; Behera, S.K.; Chakrabortty, S.; Tripathy, S.K.; Ali Khan, M.; Kumar, R.; Jeon, B.-H.; et al. Sprayable biogenic Ag-collagen nanocomposites with potent antibacterial and antibiofilm activity for *Acinetobacter baumannii* infected wound healing under hyperglycemic condition. *Chem. Eng. J.* **2024**, *490*, 151788. [CrossRef]
5. Saleh, T.A. Nanomaterials: Classification, properties, and environmental toxicities. *Environ. Technol. Innov.* **2020**, *20*, 101067. [CrossRef]
6. Aljuhani, E.; Al-Ahmed, Z.A. Evaluation of the physical parameters of nano-sized tetrachlorosilane as an inorganic material a mixed solvent using Fuoss-Shedlovsky and Fuoss-Hsia-Fernandez-Prini techniques. Biointerface Res. *Appl. Chem.* **2020**, *10*, 5741–5746.
7. Ejtemaee, P.; Khamehchi, E. Experimental investigation of rheological properties and formation damage of water-based drilling fluids in the presence of Al_2O_3, Fe_3O_4, and TiO_2 nanoparticles. *Biointerface Res. Appl. Chem* **2020**, *10*, 5886–5894.
8. Zhao, C.-X.; He, L.; Qiao, S.Z.; Middelberg, A.P. Nanoparticle synthesis in microreactors. *Chem. Eng. Sci.* **2011**, *66*, 1463–1479. [CrossRef]
9. Whitesides, G.M. The origins and the future of microfluidics. *Nature* **2006**, *442*, 368–373. [CrossRef]

10. Agha, A.; Waheed, W.; Stiharu, I.; Nerguizian, V.; Destgeer, G.; Abu-Nada, E.; Alazzam, A. A review on microfluidic-assisted nanoparticle synthesis, and their applications using multiscale simulation methods. *Discov. Nano* **2023**, *18*, 18. [CrossRef]
11. Bally, F.; Serra, C.A.; Hessel, V.; Hadziioannou, G. Micromixer-assisted polymerization processes. *Chem. Eng. Sci.* **2011**, *66*, 1449–1462. [CrossRef]
12. Olanrewaju, A.; Beaugrand, M.; Yafia, M.; Juncker, D. Capillary microfluidics in microchannels: From microfluidic networks to capillaric circuits. *Lab Chip* **2018**, *18*, 2323–2347. [CrossRef] [PubMed]
13. Hwang, J.; Cho, Y.H.; Park, M.S.; Kim, B.H. Microchannel fabrication on glass materials for microfluidic devices. *Int. J. Precis. Eng. Manuf.* **2019**, *20*, 479–495. [CrossRef]
14. Preetam, S.; Nahak, B.K.; Patra, S.; Toncu, D.C.; Park, S.; Syväjärvi, M.; Orive, G.; Tiwari, A. Emergence of microfluidics for next generation biomedical devices. *Biosens. Bioelectron. X* **2022**, *10*, 100106. [CrossRef]
15. Lai, X.; Lu, B.; Zhang, P.; Zhang, X.; Pu, Z.; Yu, H.; Li, D. Sticker microfluidics: A method for fabrication of customized monolithic microfluidics. *ACS Biomater. Sci. Eng.* **2019**, *5*, 6801–6810. [CrossRef]
16. Ma, J.; Lee, S.M.-Y.; Yi, C.; Li, C.-W. Controllable synthesis of functional nanoparticles by microfluidic platforms for biomedical applications–a review. *Lab Chip* **2017**, *17*, 209–226. [CrossRef]
17. Shrimal, P.; Jadeja, G.; Patel, S. A review on novel methodologies for drug nanoparticle preparation: Microfluidic approach. *Chem. Eng. Res. Des.* **2020**, *153*, 728–756. [CrossRef]
18. Sebastian Cabeza, V. *Chapter High and Efficient Production of Nanomaterials by Microfluidic Reactor Approaches*; InTechOpen: London, UK, 2016.
19. Huang, Y.; Liu, C.; Feng, Q.; Sun, J. Microfluidic synthesis of nanomaterials for biomedical applications. *Nanoscale Horiz.* **2023**, *8*, 610–1627. [CrossRef]
20. Kamat, V.; Dey, P.; Bodas, D.; Kaushik, A.; Boymelgreen, A.; Bhansali, S. Active microfluidic reactor-assisted controlled synthesis of nanoparticles and related potential biomedical applications. *J. Mater. Chem. B* **2023**, *11*, 5650–5667. [CrossRef]
21. Almeida, D.R.; Gil, J.F.; Guillot, A.J.; Li, J.; Pinto, R.J.; Santos, H.A.; Gonçalves, G. Advances in Microfluidic-based Core@ Shell Nanoparticles Fabrication for Cancer Applications. *Adv. Healthcare Mater.* **2024**, *13*, 2400946. [CrossRef]
22. Udepurkar, A.P.; Mampaey, L.; Clasen, C.; Cabeza, V.S.; Kuhn, S. Microfluidic synthesis of PLGA nanoparticles enabled by an ultrasonic microreactor. *React. Chem. Eng.* **2024**, *9*, 2208–2217. [CrossRef]
23. Mehraji, S.; DeVoe, D.L. Microfluidic synthesis of lipid-based nanoparticles for drug delivery: Recent advances and opportunities. *Lab Chip* **2024**, *24*, 1154–1174. [CrossRef] [PubMed]
24. Chircov, C.; Dumitru, I.A.; Vasile, B.S.; Oprea, O.-C.; Holban, A.M.; Popescu, R.C. Microfluidic Synthesis of Magnetite Nanoparticles for the Controlled Release of Antibiotics. *Pharmaceutics* **2023**, *15*, 2215. [CrossRef] [PubMed]
25. Saikia, A.; Newar, R.; Das, S.; Singh, A.; Deuri, D.J.; Baruah, A. Scopes and challenges of microfluidic technology for nanoparticle synthesis, photocatalysis and sensor applications: A comprehensive review. *Chem. Eng. Res. Des.* **2023**, *193*, 516–539. [CrossRef]
26. Zhang, Y.-F.; Zhang, S.; Zhan, L.-W.; Tang, W.-Y.; Hou, J.; Li, B.-D. Application of microfluidic technology on preparation of nano LLM-105. *J. Energetic Mater.* **2024**, *42*, 391–405. [CrossRef]
27. Niculescu, A.-G.; Mihaiescu, D.E.; Grumezescu, A.M. A review of microfluidic experimental designs for nanoparticle synthesis. *Int. J. Mol. Sci.* **2022**, *23*, 8293. [CrossRef]
28. Khizar, S.; Zine, N.; Errachid, A.; Jaffrezic-Renault, N.; Elaissari, A. Microfluidic-based nanoparticle synthesis and their potential applications. *Electrophoresis* **2022**, *43*, 819–838. [CrossRef]
29. Hamdallah, S.I.; Zoqlam, R.; Erfle, P.; Blyth, M.; Alkilany, A.M.; Dietzel, A.; Qi, S. Microfluidics for pharmaceutical nanoparticle fabrication: The truth and the myth. *Int. J. Pharm.* **2020**, *584*, 119408. [CrossRef]
30. Liu, Y.; Jiang, X. Why microfluidics? Merits and trends in chemical synthesis. *Lab Chip* **2017**, *17*, 3960–3978. [CrossRef]
31. Augustine, R.; Hasan, A. Multimodal applications of phytonanoparticles. In *Phytonanotechnology*; Elsevier: Amsterdam, The Netherlands, 2020; pp. 195–219.
32. Chatterjee, A.; Kwatra, N.; Abraham, J. Nanoparticles fabrication by plant extracts. In *Phytonanotechnology*; Elsevier: Amsterdam, The Netherlands, 2020; pp. 143–157.
33. Fajar, M.N.; Endarko, E.; Rubiyanto, A.; Malek, N.A.N.N.; Hadibarata, T.; Syafiuddin, A. A green deposition method of silver nanoparticles on textiles and their antifungal activity. *Biointerface Res. Appl. Chem.* **2020**, *10*, 4902–4907.
34. Fahmy, A.; Zaid, H.; Ibrahim, M. Optimizing the electrospun parameters which affect the preparation of nanofibers. *Biointerface Res. Appl. Chem* **2019**, *9*, 4463–4473.
35. Liu, D.; Cito, S.; Zhang, Y.; Wang, C.F.; Sikanen, T.M.; Santos, H.A. A versatile and robust microfluidic platform toward high throughput synthesis of homogeneous nanoparticles with tunable properties. *Adv. Mater.* **2015**, *27*, 2298–2304. [CrossRef] [PubMed]
36. Yang, Y.A.; Wu, H.; Williams, K.R.; Cao, Y.C. Synthesis of CdSe and CdTe nanocrystals without precursor injection. *Angew. Chem. Int. Ed.* **2005**, *44*, 6712–6715. [CrossRef] [PubMed]
37. Liu, D.; Bernuz, C.R.; Fan, J.; Li, W.; Correia, A.; Hirvonen, J.; Santos, H.A. A nano-in-nano vector: Merging the best of polymeric nanoparticles and drug nanocrystals. *Adv. Funct. Mater.* **2017**, *27*, 1604508. [CrossRef]
38. Ahmed, B.S.; Mostafa, A.A.; Darwesh, O.M.; Abdel-Rahim, E.A. Development of specific nano-antibody for application in selective and rapid environmental diagnoses of Salmonella arizonae. *Biointerface Res. Appl. Chem.* **2020**, *10*, 7198–7208.

39. Monajjemi, M.; Naghsh, F.; Mollaamin, F. Bio-lipid nano capacitors: Resonance with helical myeline proteins. *Biointerface Res. Appl. Chem* **2020**, *10*, 6695–6705.
40. Zhao, X.; Bian, F.; Sun, L.; Cai, L.; Li, L.; Zhao, Y. Microfluidic generation of nanomaterials for biomedical applications. *Small* **2020**, *16*, 1901943. [CrossRef]
41. Niculescu, A.-G.; Chircov, C.; Bîrcă, A.C.; Grumezescu, A.M. Nanomaterials synthesis through microfluidic methods: An updated overview. *Nanomaterials* **2021**, *11*, 864. [CrossRef]
42. Baig, N.; Kammakakam, I.; Falath, W. Nanomaterials: A review of synthesis methods, properties, recent progress, and challenges. *Mater. Adv.* **2021**, *2*, 1821–1871. [CrossRef]
43. Sabdono, P.; Sustiawan, F.; Fadlillah, D.A. The effect of nano-cement content to the compressive strength of mortar. *Procedia Eng.* **2014**, *95*, 386–395. [CrossRef]
44. Shah, M.; Sahoo, K.L.; Das, S.K.; Das, G. Wear mechanism of high chromium white cast iron and its microstructural evolutions during the comminution process. *Tribol. Lett.* **2020**, *68*, 77. [CrossRef]
45. Benjamin, J.S. Mechanical alloying—A perspective. *Met. Powder Rep.* **1990**, *45*, 122–127. [CrossRef]
46. Zhang, D.; Bi, H.; Liu, B.; Qiao, L. Detection of pathogenic microorganisms by microfluidics based analytical methods. *Anal. Chem.* **2018**, *90*, 5512–5520. [CrossRef] [PubMed]
47. Mei, Q.; Lu, K. Melting and superheating of crystalline solids: From bulk to nanocrystals. *Prog. Mater. Sci.* **2007**, *52*, 1175–1262. [CrossRef]
48. Jia, Y.; Yang, C.; Chen, X.; Xue, W.; Hutchins-Crawford, H.J.; Yu, Q.; Topham, P.D.; Wang, L. A review on electrospun magnetic nanomaterials: Methods, properties and applications. *J. Mater. Chem. C* **2021**, *9*, 9042–9082. [CrossRef]
49. Song, X.; Cheng, G.; Cheng, B.; Xing, J. Electrospun polyacrylonitrile/magnetic Fe_3O_4–polyhedral oligomeric silsesquioxanes nanocomposite fibers with enhanced filter performance for electrets filter media. *J. Mater. Res.* **2016**, *31*, 2662–2671. [CrossRef]
50. Cheng, C.; Dai, J.; Li, Z.; Feng, W. Preparation and magnetic properties of $CoFe_2O_4$ oriented fiber arrays by electrospinning. *Materials* **2020**, *13*, 3860. [CrossRef]
51. Kumar, P.S.; Sundaramurthy, J.; Sundarrajan, S.; Babu, V.J.; Singh, G.; Allakhverdiev, S.I.; Ramakrishna, S. Hierarchical electrospun nanofibers for energy harvesting, production and environmental remediation. *Energy Environ. Sci.* **2014**, *7*, 3192–3222.
52. Du, P.; Song, L.; Xiong, J.; Li, N.; Xi, Z.; Wang, L.; Jin, D.; Guo, S.; Yuan, Y. Coaxial electrospun TiO_2/ZnO core–sheath nanofibers film: Novel structure for photoanode of dye-sensitized solar cells. *Electrochim. Acta* **2012**, *78*, 392–397. [CrossRef]
53. Paramasivam, G.; Palem, V.V.; Sundaram, T.; Sundaram, V.; Kishore, S.C.; Bellucci, S. Nanomaterials: Synthesis and applications in theranostics. *Nanomaterials* **2021**, *11*, 3228. [CrossRef]
54. Qu, C.; Kinzel, E.C. Infrared metasurfaces created with off-normal incidence microsphere photolithography. *Opt. Express* **2017**, *25*, 12632–12639. [CrossRef]
55. Kuo, C.W.; Shiu, J.Y.; Cho, Y.H.; Chen, P. Fabrication of large-area periodic nanopillar arrays for nanoimprint lithography using polymer colloid masks. *Adv. Mater.* **2003**, *15*, 1065–1068. [CrossRef]
56. Yin, Y.; Gates, B.; Xia, Y. A soft lithography approach to the fabrication of nanostructures of single crystalline silicon with well-defined dimensions and shapes. *Adv. Mater.* **2000**, *12*, 1426–1430. [CrossRef]
57. Crivellaro, S.; Guadagnini, A.; Arboleda, D.M.; Schinca, D.; Amendola, V. A system for the synthesis of nanoparticles by laser ablation in liquid that is remotely controlled with PC or smartphone. *Rev. Sci. Instrum.* **2019**, *90*, 033902. [CrossRef] [PubMed]
58. Kim, M.; Osone, S.; Kim, T.; Higashi, H.; Seto, T. Synthesis of nanoparticles by laser ablation: A review. *KONA Powder Part. J.* **2017**, *34*, 80–90. [CrossRef]
59. Alheshibri, M. Fabrication of Au–Ag bimetallic nanoparticles using pulsed laser ablation for medical applications: A review. *Nanomaterials* **2023**, *13*, 2940. [CrossRef]
60. Duque, J.S.; Madrigal, B.M.; Riascos, H.; Avila, Y.P. Colloidal metal oxide nanoparticles prepared by laser ablation technique and their antibacterial test. *Colloids Interfaces* **2019**, *3*, 25. [CrossRef]
61. Park, H.; Reddy, D.A.; Kim, Y.; Lee, S.; Ma, R.; Kim, T.K. Synthesis of ultra-small palladium nanoparticles deposited on CdS nanorods by pulsed laser ablation in liquid: Role of metal nanocrystal size in the photocatalytic hydrogen production. *Chem.–A Eur. J.* **2017**, *23*, 13112–13119. [CrossRef]
62. Son, H.H.; Seo, G.H.; Jeong, U.; Kim, S.J. Capillary wicking effect of a Cr-sputtered superhydrophilic surface on enhancement of pool boiling critical heat flux. *Int. J. Heat Mass Transf.* **2017**, *113*, 115–128. [CrossRef]
63. Wender, H.; Migowski, P.; Feil, A.F.; Teixeira, S.R.; Dupont, J. Sputtering deposition of nanoparticles onto liquid substrates: Recent advances and future trends. *Coord. Chem. Rev.* **2013**, *257*, 2468–2483. [CrossRef]
64. Muñoz-García, J.; Vázquez, L.; Cuerno, R.; Sánchez-García, J.; Castro, M.; Gago, R.; Wang, Z. *Toward Functional Nanomaterials*; Wang, Z.W., Ed.; Springer: Dordrecht, The Netherlands, 2009; p. 323.
65. Nam, J.H.; Jang, M.J.; Jang, H.Y.; Park, W.; Wang, X.; Choi, S.M.; Cho, B. Room-temperature sputtered electrocatalyst WSe_2 nanomaterials for hydrogen evolution reaction. *J. Energy Chem.* **2020**, *47*, 107–111. [CrossRef]
66. Nie, M.; Sun, K.; Meng, D.D. Formation of metal nanoparticles by short-distance sputter deposition in a reactive ion etching chamber. *J. Appl. Phys.* **2009**, *106*, 054314. [CrossRef]
67. Zhang, D.; Zhang, K.; Yao, Y.; Liang, F.; Qu, T.; Ma, W.; Yang, B.; Dai, Y.; Lei, Y. Intercalation and exfoliation syntheses of high specific surface area graphene and FeC_2O_4/graphene composite for anode material of lithium ion battery. *Fuller. Nanotub. Carbon Nanostruct.* **2019**, *27*, 746–754. [CrossRef]

68. Liehr, A.D. Solid State Physics. Advances in Research and Applications. *J. Am. Chem. Soc.* **1960**, *82*, 2658–2659. [CrossRef]
69. Liang, F.; Tanaka, M.; Choi, S.; Watanabe, T. Formation of different arc-anode attachment modes and their effect on temperature fluctuation for carbon nanomaterial production in DC arc discharge. *Carbon* **2017**, *117*, 100–111. [CrossRef]
70. Liang, F.; Shimizu, T.; Tanaka, M.; Choi, S.; Watanabe, T. Selective preparation of polyhedral graphite particles and multi-wall carbon nanotubes by a transferred arc under atmospheric pressure. *Diam. Relat. Mater.* **2012**, *30*, 70–76. [CrossRef]
71. Li, N.; Wang, Z.; Zhao, K.; Shi, Z.; Gu, Z.; Xu, S. Synthesis of single-wall carbon nanohorns by arc-discharge in air and their formation mechanism. *Carbon* **2010**, *48*, 1580–1585. [CrossRef]
72. Wu, Z.-S.; Ren, W.; Gao, L.; Zhao, J.; Chen, Z.; Liu, B.; Tang, D.; Yu, B.; Jiang, C.; Cheng, H.-M. Synthesis of graphene sheets with high electrical conductivity and good thermal stability by hydrogen arc discharge exfoliation. *ACS Nano* **2009**, *3*, 411–417. [CrossRef]
73. Dion, C.D.; Tavares, J.R. Photo-initiated chemical vapor deposition as a scalable particle functionalization technology (a practical review). *Powder Technol.* **2013**, *239*, 484–491. [CrossRef]
74. Jones, A.C.; Hitchman, M.L. Overview of chemical vapour deposition. *Chem. Vap. Depos. Precursors Process. Appl.* **2009**, *1*, 1–36.
75. Mandracci, P. *Chemical Vapor Deposition for Nanotechnology*; IntechOpen: London, UK, 2019.
76. Parashar, M.; Shukla, V.K.; Singh, R. Metal oxides nanoparticles via sol–gel method: A review on synthesis, characterization and applications. *J. Mater. Sci. Mater. Electron.* **2020**, *31*, 3729–3749. [CrossRef]
77. Bokov, D.; Turki Jalil, A.; Chupradit, S.; Suksatan, W.; Javed Ansari, M.; Shewael, I.H.; Valiev, G.H.; Kianfar, E. Nanomaterial by sol-gel method: Synthesis and application. *Adv. Mater. Sci. Eng.* **2021**, *2021*, 5102014. [CrossRef]
78. Gupta, S.M.; Tripathi, M. A review on the synthesis of TiO_2 nanoparticles by solution route. *Cent. Eur. J. Chem.* **2012**, *10*, 279–294. [CrossRef]
79. Arya, S.; Mahajan, P.; Mahajan, S.; Khosla, A.; Datt, R.; Gupta, V.; Young, S.-J.; Oruganti, S.K. Influence of processing parameters to control morphology and optical properties of Sol-Gel synthesized ZnO nanoparticles. *ECS J. Solid State Sci. Technol.* **2021**, *10*, 023002. [CrossRef]
80. Ristić, M.; Musić, S.; Ivanda, M.; Popović, S. Sol–gel synthesis and characterization of nanocrystalline ZnO powders. *J. Alloys Compd.* **2005**, *397*, L1–L4. [CrossRef]
81. Yue, S.; Yan, Z.; Shi, Y.; Ran, G. Synthesis of zinc oxide nanotubes within ultrathin anodic aluminum oxide membrane by sol–gel method. *Mater. Lett.* **2013**, *98*, 246–249. [CrossRef]
82. Lakshmi, B.B.; Dorhout, P.K.; Martin, C.R. Sol−gel template synthesis of semiconductor nanostructures. *Chem. Mater.* **1997**, *9*, 857–862. [CrossRef]
83. Lone, I.H.; Radwan, N.R.; Aslam, J.; Akhter, A. Concept of reverse micelle method for the synthesis of nano-structured materials. *Curr. Nanosci.* **2019**, *15*, 129–136. [CrossRef]
84. Ghosh, S. Comparative studies on brij reverse micelles prepared in benzene/surfactant/ethylammonium nitrate systems: Effect of head group size and polarity of the hydrocarbon chain. *J. Colloid Interface Sci.* **2011**, *360*, 672–680. [CrossRef]
85. Nasi, R.; Esposito, S.; Freyria, F.S.; Armandi, M.; Gadhi, T.A.; Hernandez, S.; Rivolo, P.; Ditaranto, N.; Bonelli, B. Application of reverse micelle sol–gel synthesis for bulk doping and heteroatoms surface enrichment in mo-doped TiO_2 nanoparticles. *Materials* **2019**, *12*, 937. [CrossRef]
86. Chandra, P.; Doke, D.S.; Umbarkar, S.B.; Biradar, A.V. One-pot synthesis of ultrasmall MoO_3 nanoparticles supported on SiO_2, TiO_2, and ZrO_2 nanospheres: An efficient epoxidation catalyst. *J. Mater. Chem. A* **2014**, *2*, 19060–19066. [CrossRef]
87. Liu, Y.; Goebl, J.; Yin, Y. Themed issue: Chemistry of functional nanomaterials. *Chem. Soc. Rev* **2013**, *42*, 2610–2653. [CrossRef] [PubMed]
88. Li, W.; Zhao, D. An overview of the synthesis of ordered mesoporous materials. *Chem. Commun.* **2013**, *49*, 943–946. [CrossRef] [PubMed]
89. Poolakkandy, R.R.; Menamparambath, M.M. Soft-template-assisted synthesis: A promising approach for the fabrication of transition metal oxides. *Nanoscale Adv.* **2020**, *2*, 5015–5045. [CrossRef] [PubMed]
90. Liu, J.; Yang, T.; Wang, D.-W.; Lu, G.Q.; Zhao, D.; Qiao, S.Z. A facile soft-template synthesis of mesoporous polymeric and carbonaceous nanospheres. *Nat. Commun.* **2013**, *4*, 2798. [CrossRef]
91. Tang, T.; Zhang, T.; Li, W.; Huang, X.; Wang, X.; Qiu, H.; Hou, Y. Mesoporous N-doped graphene prepared by a soft-template method with high performance in Li–S batteries. *Nanoscale* **2019**, *11*, 7440–7446. [CrossRef]
92. Szczęśniak, B.; Choma, J.; Jaroniec, M. Major advances in the development of ordered mesoporous materials. *Chem. Commun.* **2020**, *56*, 7836–7848. [CrossRef]
93. Hurst, S.J.; Payne, E.K.; Qin, L.; Mirkin, C.A. Multisegmented one-dimensional nanorods prepared by hard-template synthetic methods. *Angew. Chem. Int. Ed.* **2006**, *45*, 2672–2692. [CrossRef]
94. Kumar, M.; Xiong, X.; Wan, Z.; Sun, Y.; Tsang, D.C.; Gupta, J.; Gao, B.; Cao, X.; Tang, J.; Ok, Y.S. Ball milling as a mechanochemical technology for fabrication of novel biochar nanomaterials. *Bioresour. Technol.* **2020**, *312*, 123613. [CrossRef]
95. Schrittwieser, S.; Haslinger, M.J.; Mitteramskogler, T.; Mühlberger, M.; Shoshi, A.; Brückl, H.; Bauch, M.; Dimopoulos, T.; Schmid, B.; Schotter, J. Multifunctional nanostructures and nanopocket particles fabricated by nanoimprint lithography. *Nanomaterials* **2019**, *9*, 1790. [CrossRef]
96. Chakrabartty, I.; Hakeem, K.R.; Mohanta, Y.K.; Varma, R.S. Greener nanomaterials and their diverse applications in the energy sector. *Clean Technol. Environ.* **2022**, *24*, 3237–3252. [CrossRef]

97. Gu, F.; Wang, S.F.; Song, C.F.; Lü, M.K.; Qi, Y.X.; Zhou, G.J.; Xu, D.; Yuan, D.R. Synthesis and luminescence properties of SnO_2 nanoparticles. *Chem. Phys. Lett.* **2003**, *372*, 451–454. [CrossRef]
98. Mahato, T.; Prasad, G.; Singh, B.; Acharya, J.; Srivastava, A.; Vijayaraghavan, R. Nanocrystalline zinc oxide for the decontamination of sarin. *J. Hazard. Mater.* **2009**, *165*, 928–932. [CrossRef] [PubMed]
99. Wang, X.; Li, J.-G.; Kamiyama, H.; Ishigaki, T. Fe-doped TiO_2 nanopowders by oxidative pyrolysis of organometallic precursors in induction thermal plasma: Synthesis and structural characterization. *Thin Solid Films* **2006**, *506*, 278–282. [CrossRef]
100. Zhang, L.; Chen, Q.; Ma, Y.; Sun, J. Microfluidic methods for fabrication and engineering of nanoparticle drug delivery systems. *ACS Appl. Bio Mater.* **2019**, *3*, 107–120. [CrossRef]
101. Ren, K.; Zhou, J.; Wu, H. Materials for microfluidic chip fabrication. *Acc. Chem. Res.* **2013**, *46*, 2396–2406. [CrossRef]
102. Liao, S.; He, Y.; Chu, Y.; Liao, H.; Wang, Y. Solvent-resistant and fully recyclable perfluoropolyether-based elastomer for microfluidic chip fabrication. *J. Mater. Chem. A* **2019**, *7*, 16249–16256. [CrossRef]
103. Nielsen, J.B.; Hanson, R.L.; Almughamsi, H.M.; Pang, C.; Fish, T.R.; Woolley, A.T. Microfluidics: Innovations in materials and their fabrication and functionalization. *Anal. Chem.* **2019**, *92*, 150–168. [CrossRef]
104. Guckenberger, D.J.; De Groot, T.E.; Wan, A.M.; Beebe, D.J.; Young, E.W. Micromilling: A method for ultra-rapid prototyping of plastic microfluidic devices. *Lab Chip* **2015**, *15*, 2364–2378. [CrossRef]
105. Waldbaur, A.; Rapp, H.; Länge, K.; Rapp, B.E. Let there be chip—Towards rapid prototyping of microfluidic devices: One-step manufacturing processes. *Anal. Methods* **2011**, *3*, 2681–2716. [CrossRef]
106. Carrell, C.; Kava, A.; Nguyen, M.; Menger, R.; Munshi, Z.; Call, Z.; Nussbaum, M.; Henry, C. Beyond the lateral flow assay: A review of paper-based microfluidics. *Microelectron. Eng.* **2019**, *206*, 45–54. [CrossRef]
107. Sachdeva, S.; Davis, R.W.; Saha, A.K. Microfluidic point-of-care testing: Commercial landscape and future directions. *Front. Bioeng. Biotechnol.* **2021**, *8*, 602659. [CrossRef] [PubMed]
108. Tian, F.; Cai, L.; Chang, J.; Li, S.; Liu, C.; Li, T.; Sun, J. Label-free isolation of rare tumor cells from untreated whole blood by interfacial viscoelastic microfluidics. *Lab Chip* **2018**, *18*, 3436–3445. [CrossRef] [PubMed]
109. Zhang, L.; Ding, B.; Chen, Q.; Feng, Q.; Lin, L.; Sun, J. Point-of-care-testing of nucleic acids by microfluidics. *TrAC Trends Anal. Chem.* **2017**, *94*, 106–116. [CrossRef]
110. Belliveau, N.M.; Huft, J.; Lin, P.J.; Chen, S.; Leung, A.K.; Leaver, T.J.; Wild, A.W.; Lee, J.B.; Taylor, R.J.; Tam, Y.K. Microfluidic synthesis of highly potent limit-size lipid nanoparticles for in vivo delivery of siRNA. *Molecular Therapy-Nucleic Acids* **2012**, *1*, e37. [CrossRef]
111. Valencia, P.M.; Farokhzad, O.C.; Karnik, R.; Langer, R. Microfluidic technologies for accelerating the clinical translation of nanoparticles. In *Nano-Enabled Medical Applications*; Jenny Stanford Publishing: Singapore, 2020; pp. 93–112.
112. Valencia, P.M.; Pridgen, E.M.; Rhee, M.; Langer, R.; Farokhzad, O.C.; Karnik, R. Microfluidic platform for combinatorial synthesis and optimization of targeted nanoparticles for cancer therapy. *ACS Nano* **2013**, *7*, 10671–10680. [CrossRef]
113. Zhang, S.; Gao, H.; Bao, G. Physical principles of nanoparticle cellular endocytosis. *ACS Nano* **2015**, *9*, 8655–8671. [CrossRef]
114. Kimura, N.; Maeki, M.; Sato, Y.; Note, Y.; Ishida, A.; Tani, H.; Harashima, H.; Tokeshi, M. Development of the iLiNP device: Fine tuning the lipid nanoparticle size within 10 nm for drug delivery. *ACS Omega* **2018**, *3*, 5044–5051. [CrossRef]
115. Thiermann, R.; Mueller, W.; Montesinos-Castellanos, A.; Metzke, D.; Löb, P.; Hessel, V.; Maskos, M. Size controlled polymersomes by continuous self-assembly in micromixers. *Polymer* **2012**, *53*, 2205–2210. [CrossRef]
116. Mijajlovic, M.; Wright, D.; Zivkovic, V.; Bi, J.; Biggs, M. Microfluidic hydrodynamic focusing based synthesis of POPC liposomes for model biological systems. *Colloids Surf. B Biointerfaces* **2013**, *104*, 276–281. [CrossRef]
117. Gunduz, O.; Ahmad, Z.; Stride, E.; Edirisinghe, M. Continuous generation of ethyl cellulose drug delivery nanocarriers from microbubbles. *Pharm. Res.* **2013**, *30*, 225–237. [CrossRef]
118. Zhang, L.; Feng, Q.; Wang, J.; Zhang, S.; Ding, B.; Wei, Y.; Dong, M.; Ryu, J.-Y.; Yoon, T.-Y.; Shi, X. Microfluidic synthesis of hybrid nanoparticles with controlled lipid layers: Understanding flexibility-regulated cell–nanoparticle interaction. *ACS Nano* **2015**, *9*, 9912–9921. [CrossRef] [PubMed]
119. He, Y.; Park, K. Effects of the microparticle shape on cellular uptake. *Mol. Pharm.* **2016**, *13*, 2164–2171. [CrossRef] [PubMed]
120. Dashtimoghadam, E.; Mirzadeh, H.; Taromi, F.A.; Nyström, B. Microfluidic self-assembly of polymeric nanoparticles with tunable compactness for controlled drug delivery. *Polymer* **2013**, *54*, 4972–4979. [CrossRef]
121. Hui, Y.; Yi, X.; Hou, F.; Wibowo, D.; Zhang, F.; Zhao, D.; Gao, H.; Zhao, C.-X. Role of nanoparticle mechanical properties in cancer drug delivery. *ACS Nano* **2019**, *13*, 7410–7424. [CrossRef]
122. Feng, Q.; Liu, J.; Li, X.; Chen, Q.; Sun, J.; Shi, X.; Ding, B.; Yu, H.; Li, Y.; Jiang, X. One-step microfluidic synthesis of nanocomplex with tunable rigidity and acid-switchable surface charge for overcoming drug resistance. *Small* **2017**, *13*, 1603109. [CrossRef]
123. Di Santo, R.; Digiacomo, L.; Palchetti, S.; Palmieri, V.; Perini, G.; Pozzi, D.; Papi, M.; Caracciolo, G. Microfluidic manufacturing of surface-functionalized graphene oxide nanoflakes for gene delivery. *Nanoscale* **2019**, *11*, 2733–2741. [CrossRef]
124. Damiati, S.; Kompella, U.B.; Damiati, S.A.; Kodzius, R. Microfluidic devices for drug delivery systems and drug screening. *Genes* **2018**, *9*, 103. [CrossRef]
125. Yu, B.; Lee, R.J.; Lee, L.J. Microfluidic methods for production of liposomes. *Methods Enzymol.* **2009**, *465*, 129–141.
126. Fick, A. Ueber Diffusion. *Ann. Der Phys.* **1855**, *170*, 59–86. [CrossRef]
127. Reynolds, O. XXIX. An experimental investigation of the circumstances which determine whether the motion of water shall be direct or sinuous, and of the law of resistance in parallel channels. *Philos. Trans. R. Soc. Lond.* **1997**, *174*, 935–982. [CrossRef]

128. Wang, C.-T.; Hu, Y.-C.; Hu, T.-Y. Biophysical Micromixer. *Sensors* **2009**, *9*, 5379–5389. [CrossRef] [PubMed]
129. Gimondi, S.; Ferreira, H.; Reis, R.L.; Neves, N.M. Microfluidic devices: A tool for nanoparticle synthesis and performance evaluation. *ACS Nano* **2023**, *17*, 14205–14228. [CrossRef] [PubMed]
130. Rasouli, M.R.; Tabrizian, M. An ultra-rapid acoustic micromixer for synthesis of organic nanoparticles. *Lab Chip* **2019**, *19*, 3316–3325. [CrossRef] [PubMed]
131. Hong, S.O.; Park, K.-S.; Kim, D.-Y.; Lee, S.S.; Lee, C.-S.; Kim, J.M. Gear-shaped micromixer for synthesis of silica particles utilizing inertio-elastic flow instability. *Lab Chip* **2021**, *21*, 513–520. [CrossRef]
132. Singh, A.D.; Limaye, M.V.; Singh, S.B.; Lalla, N.P.; Malek, C.K.; Kulkarni, S.K. A facile and fast approach for the synthesis of doped nanoparticles using a microfluidic device. *Nanotechnology* **2008**, *19*, 245613. [CrossRef]
133. Chen, X.; Arruebo, M.; Yeung, K.L. Flow-synthesis of mesoporous silicas and their use in the preparation of magnetic catalysts for Knoevenagel condensation reactions. *Catal. Today* **2013**, *204*, 140–147. [CrossRef]
134. Han, S.-Y.; Paul, B.K.; Chang, C.-h. Nanostructured ZnO as biomimetic anti-reflective coatings on textured silicon using a continuous solution process. *J. Mater. Chem.* **2012**, *22*, 22906–22912. [CrossRef]
135. Wang, X.; Liu, Z.; Cai, Y.; Song, Q.; Wang, B. Synthesis of Cu_2O Nanoparticles by Ellipse Curve Micromixer. *ACS Omega* **2023**, *8*, 29758–29769. [CrossRef]
136. Chang, M.; Gabayno, J.L.F.; Ye, R.; Huang, K.-W.; Chang, Y.-J. Mixing efficiency enhancing in micromixer by controlled magnetic stirring of Fe_3O_4 nanomaterial. *Microsyst. Technol.* **2017**, *23*, 457–463. [CrossRef]
137. Patil, G.A.; Bari, M.L.; Bhanvase, B.A.; Ganvir, V.; Mishra, S.; Sonawane, S.H. Continuous synthesis of functional silver nanoparticles using microreactor: Effect of surfactant and process parameters. *Chem. Eng. Process. Process Intensif.* **2012**, *62*, 69–77. [CrossRef]
138. Song, Y.; Li, R.; Sun, Q.; Jin, P. Controlled growth of Cu nanoparticles by a tubular microfluidic reactor. *Chem. Eng. J.* **2011**, *168*, 477–484. [CrossRef]
139. Liu, G.; Li, Z.; Li, X.; Luo, Y.; Wang, X.; Zhu, D.; Yang, Z.; Wang, J. Controllable Synthesis of Silver Nanoparticles Using a Double-Layer Y-Shaped SAR Micromixer. *Nano* **2020**, *15*, 2050068. [CrossRef]
140. Magdalene, D.J.; Muthuselvam, D.; Pravinraj, T. Microfluidics-based green synthesis of silver nanoparticle from the aqueous leaf extract of *Ipomea quamoclit* L. *Appl. Nanosci.* **2021**, *11*, 2073–2084. [CrossRef]
141. Maged, A.; Abdelbaset, R.; Mahmoud, A.A.; Elkasabgy, N.A. Merits and advances of microfluidics in the pharmaceutical field: Design technologies and future prospects. *Drug Deliv.* **2022**, *29*, 1549–1570. [CrossRef] [PubMed]
142. Cai, G.; Xue, L.; Zhang, H.; Lin, J. A Review on Micromixers. *Micromachines* **2017**, *8*, 274. [CrossRef]
143. Tata Rao, L.; Goel, S.; Kumar Dubey, S.; Javed, A. Performance Investigation of T-Shaped Micromixer with Different Obstacles. *J. Phys. Conf. Ser.* **2019**, *1276*, 012003. [CrossRef]
144. Niculescu, A.-G.; Munteanu, O.M.; Bîrcă, A.C.; Moroșan, A.; Purcăreanu, B.; Vasile, B.Ș.; Istrati, D.; Mihaiescu, D.E.; Hadibarata, T.; Grumezescu, A.M. New 3D Vortex Microfluidic System Tested for Magnetic Core-Shell Fe_3O_4-SA Nanoparticle Synthesis. *Nanomaterials* **2024**, *14*, 902. [CrossRef]
145. Jahangir, R.; Munir, I.; Yesiloz, G. One-Step Synthesis of Ultrasmall Nanoparticles in Glycerol as a Promising Green Solvent at Room Temperature Using Omega-Shaped Microfluidic Micromixers. *Anal Chem* **2023**, *95*, 17177–17186. [CrossRef]
146. Guo, K.; Chen, Y.; Zhou, Z.; Zhu, S.; Ni, Z.; Xiang, N. A novel 3D Tesla valve micromixer for efficient mixing and chitosan nanoparticle production. *Electrophoresis* **2022**, *43*, 2184–2194. [CrossRef]
147. Zeng, C.; Wang, C.; Wang, F.; Zhang, Y.; Zhang, L. A novel vapor–liquid segmented flow based on solvent partial vaporization in microstructured reactor for continuous synthesis of nickel nanoparticles. *Chem. Eng. J.* **2012**, *204–206*, 48–53. [CrossRef]
148. Chung, C.K.; Shih, T.R.; Chang, C.K.; Lai, C.W.; Wu, B.H. Design and experiments of a short-mixing-length baffled microreactor and its application to microfluidic synthesis of nanoparticles. *Chem. Eng. J.* **2011**, *168*, 790–798. [CrossRef]
149. Sattari, A.; Hanafizadeh, P.; Hoorfar, M. Multiphase flow in microfluidics: From droplets and bubbles to the encapsulated structures. *Adv. Colloid Interface Sci.* **2020**, *282*, 102208. [CrossRef] [PubMed]
150. Chakraborty, I.; Ricouvier, J.; Yazhgur, P.; Tabeling, P.; Leshansky, A. Droplet generation at Hele-Shaw microfluidic T-junction. *Phys. Fluids* **2019**, *31*, 022010. [CrossRef]
151. Anna, S.L.; Bontoux, N.; Stone, H.A. Formation of dispersions using "flow focusing" in microchannels. *Appl. Phys. Lett.* **2003**, *82*, 364–366. [CrossRef]
152. Hamlington, B.D.; Steinhaus, B.; Feng, J.J.; Link, D.; Shelley, M.J.; Shen, A.Q. Liquid crystal droplet production in a microfluidic device. *Liq. Cryst.* **2007**, *34*, 861–870. [CrossRef]
153. Tanudjaja, H.J.; Hejase, C.A.; Tarabara, V.V.; Fane, A.G.; Chew, J.W. Membrane-based separation for oily wastewater: A practical perspective. *Water Res.* **2019**, *156*, 347–365. [CrossRef]
154. Nisisako, T.; Torii, T. Microfluidic large-scale integration on a chip for mass production of monodisperse droplets and particles. *Lab Chip* **2008**, *8*, 287–293. [CrossRef]
155. Kobayashi, I.; Takano, T.; Maeda, R.; Wada, Y.; Uemura, K.; Nakajima, M. Straight-through microchannel devices for generating monodisperse emulsion droplets several microns in size. *Microfluid. Nanofluid.* **2008**, *4*, 167–177. [CrossRef]
156. Wong, V.-L.; Ng, C.-A.I.; Teo, L.-R.I.; Lee, C.-W. Microfluidic Synthesis of Functional Materials as Potential Sorbents for Water Remediation and Resource Recovery. In *Advances in Microfluidic Technologies for Energy and Environmental Applications*; IntechOpen: London, UK, 2020; p. 39.

157. Ding, Y.; Howes, P.D.; deMello, A.J. Recent advances in droplet microfluidics. *Anal. Chem.* **2019**, *92*, 132–149. [CrossRef]
158. Singh, A.; Shirolkar, M.; Lalla, N.P.; Malek, C.K.; Kulkarni, S. Room temperature, water-based, microreactor synthesis of gold and silver nanoparticles. *Int. J. Nanotechnol.* **2009**, *6*, 541–551. [CrossRef]
159. Ye, Z.; Wang, K.; Lou, M.; Jia, X.; Xu, F.; Ye, G. Consecutive synthesis of gold nanobipyramids with controllable morphologies using a microfluidic platform. *Microfluid. Nanofluid.* **2020**, *24*, 1–8. [CrossRef]
160. Iyer, K.S.; Raston, C.L.; Saunders, M. Continuous flow nano-technology: Manipulating the size, shape, agglomeration, defects and phases of silver nano-particles. *Lab Chip* **2007**, *7*, 1800–1805. [CrossRef] [PubMed]
161. Kašpar, O.; Koyuncu, A.; Pittermannová, A.; Ulbrich, P.; Tokárová, V. Governing factors for preparation of silver nanoparticles using droplet-based microfluidic device. *Biomed. Microdevices* **2019**, *21*, 88. [CrossRef] [PubMed]
162. Hong, T.; Lu, A.; Liu, W.; Chen, C. Microdroplet synthesis of silver nanoparticles with controlled sizes. *Micromachines* **2019**, *10*, 274. [CrossRef]
163. Sue, K.; Kimura, K.; Arai, K. Hydrothermal synthesis of ZnO nanocrystals using microreactor. *Mater. Lett.* **2004**, *58*, 3229–3231. [CrossRef]
164. Luo, H.; Leprince-Wang, Y.; Jing, G. Tunable growth of ZnO nanostructures on the inner wall of capillary tubes. *J. Phys. Chem. C* **2019**, *123*, 7408–7415. [CrossRef]
165. Wang, H.; Nakamura, H.; Uehara, M.; Miyazaki, M.; Maeda, H. Preparation of titania particles utilizing the insoluble phase interface in a microchannel reactor. *Chem. Commun.* **2002**, *14*, 1462–1463. [CrossRef]
166. Hao, N.; Nie, Y.; Zhang, J.X. Microfluidic flow synthesis of functional mesoporous silica nanofibers with tunable aspect ratios. *Acs Sustain. Chem. Eng.* **2018**, *6*, 1522–1526. [CrossRef]
167. Hao, N.; Nie, Y.; Xu, Z.; Closson, A.B.; Usherwood, T.; Zhang, J.X. Microfluidic continuous flow synthesis of functional hollow spherical silica with hierarchical sponge-like large porous shell. *Chem. Eng. J.* **2019**, *366*, 433–438. [CrossRef]
168. Song, Y.; Modrow, H.; Henry, L.L.; Saw, C.K.; Doomes, E.; Palshin, V.; Hormes, J.; Kumar, C.S. Microfluidic synthesis of cobalt nanoparticles. *Chem. Mater.* **2006**, *18*, 2817–2827. [CrossRef]
169. Suryawanshi, P.L.; Sonawane, S.H.; Bhanvase, B.A.; Ashokkumar, M.; Pimplapure, M.S.; Gogate, P.R. Synthesis of iron oxide nanoparticles in a continuous flow spiral microreactor and Corning® advanced flow™ reactor. *Green Process. Synth.* **2018**, *7*, 1–11. [CrossRef]
170. Liu, J.; Gu, Y.; Wu, Q.; Wang, X.; Zhao, L.; DeMello, A.; Wen, W.; Tong, R.; Gong, X. Synthesis and study of CdSe QDs by a microfluidic method and via a bulk reaction. *Crystals* **2019**, *9*, 368. [CrossRef]
171. Xu, P.-F.; Liu, Z.-H.; Duan, Y.-H.; Sun, Q.; Wang, D.; Zeng, X.-F.; Wang, J.-X. Microfluidic controllable synthesis of monodispersed sulfur nanoparticles with enhanced antibacterial activities. *Chem. Eng. J.* **2020**, *398*, 125293. [CrossRef]
172. Hood, R.R.; DeVoe, D.L. High-throughput continuous flow production of nanoscale liposomes by microfluidic vertical flow focusing. *Small* **2015**, *11*, 5790–5799. [CrossRef]
173. Kawamura, J.; Kitamura, H.; Otake, Y.; Fuse, S.; Nakamura, H. Size-controllable and scalable production of liposomes using a v-shaped mixer micro-flow reactor. *Org. Process Res. Dev.* **2020**, *24*, 2122–2127. [CrossRef]
174. Huang, X.; Caddell, R.; Yu, B.; Xu, S.; Theobald, B.; Lee, L.J.; Lee, R.J. Ultrasound-enhanced microfluidic synthesis of liposomes. *Anticancer Res.* **2010**, *30*, 463–466. [CrossRef]
175. Shokoohinia, P.; Hajialyani, M.; Sadrjavadi, K.; Akbari, M.; Rahimi, M.; Khaledian, S.; Fattahi, A. Microfluidic-assisted preparation of PLGA nanoparticles for drug delivery purposes: Experimental study and computational fluid dynamic simulation. *Res. Pharm. Sci.* **2019**, *14*, 459–470.
176. Min, K.-I.; Lee, H.-J.; Kim, D.-P. Three-dimensional flash flow microreactor for scale-up production of monodisperse PEG–PLGA nanoparticles. *Lab Chip* **2014**, *14*, 3987–3992. [CrossRef]
177. Heshmatnezhad, F.; Solaimany Nazar, A.R. On-chip controlled synthesis of polycaprolactone nanoparticles using continuous-flow microfluidic devices. *J. Flow Chem.* **2020**, *10*, 533–543. [CrossRef]
178. Bicudo, R.C.S.; Santana, M.H.A. Production of hyaluronic acid (HA) nanoparticles by a continuous process inside microchannels: Effects of non-solvents, organic phase flow rate, and HA concentration. *Chem. Eng. Sci.* **2012**, *84*, 134–141. [CrossRef]